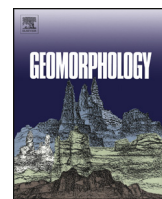




Contents lists available at ScienceDirect



Geomorphology

journal homepage: www.elsevier.com/locate/geomorph

Large-scale dam removal on the Elwha River, Washington, USA: River channel and floodplain geomorphic change

Amy E. East ^{a,*}, George R. Pess ^b, Jennifer A. Bountry ^c, Christopher S. Magirl ^d, Andrew C. Ritchie ^e, Joshua B. Logan ^a, Timothy J. Randle ^c, Mark C. Mastin ^d, Justin T. Minear ^f, Jeffrey J. Duda ^g, Martin C. Liermann ^b, Michael L. McHenry ^h, Timothy J. Beechie ^b, Patrick B. Shafroth ⁱ

^a U.S. Geological Survey, Pacific Coastal and Marine Science Center, 400 Natural Bridges Drive, Santa Cruz, CA 95060, United States^b National Marine Fisheries Service, National Oceanic and Atmospheric Administration, Seattle, WA 98112, United States^c U.S. Bureau of Reclamation, P.O. Box 25007, Mail Code 86-68240, Denver, CO 80225, United States^d U.S. Geological Survey, Washington Water Science Center, 934 Broadway, Suite 300, Tacoma, WA 94802, United States^e National Park Service, Olympic National Park, 600 E. Park Avenue, Port Angeles, WA 98362, United States^f U.S. Geological Survey, California Water Science Center, 6000 J Street, Placer Hall, Sacramento, CA 95819, United States^g U.S. Geological Survey, Western Fisheries Research Center, 6505 NE 65th St., Seattle, WA 98115, United States^h Lower Elwha Klallam Tribe, 51 Hatchery Rd., Port Angeles, WA 98363, United Statesⁱ U.S. Geological Survey, Fort Collins Science Center, 2150 Centre Ave., Bldg. C Fort Collins, CO 80526, United States

ARTICLE INFO

Article history:

Received 1 May 2014

Received in revised form 20 August 2014

Accepted 28 August 2014

Available online xxxx

Keywords:

Fluvial geomorphology

Dams

Dam removal

Channel evolution

Floodplain

Sediment wave

ABSTRACT

A substantial increase in fluvial sediment supply relative to transport capacity causes complex, large-magnitude changes in river and floodplain morphology downstream. Although sedimentary and geomorphic responses to sediment pulses are a fundamental part of landscape evolution, few opportunities exist to quantify those processes over field scales. We investigated the downstream effects of sediment released during the largest dam removal in history, on the Elwha River, Washington, USA, by measuring changes in riverbed elevation and topography, bed sediment grain size, and channel planform as two dams were removed in stages over two years. As 10.5 million t (7.1 million m³) of sediment was released from two former reservoirs, downstream dispersion of a sediment wave caused widespread bed aggradation of ~1 m (greater where pools filled), changed the river from pool-riffle to braided morphology, and decreased the slope of the lowermost river. The newly deposited sediment, which was finer than most of the pre-dam-removal bed, formed new bars (largely pebble, granule, and sand material), prompting aggradational channel avulsion that increased the channel braiding index by almost 50%. As a result of mainstem bed aggradation, floodplain channels received flow and accumulated new sediment even during low to moderate flow conditions. The river system showed a two- to tenfold greater geomorphic response to dam removal (in terms of bed elevation change magnitude) than it had to a 40-year flood event four years before dam removal. Two years after dam removal began, as the river had started to incise through deposits of the initial sediment wave, ~1.2 million t of new sediment (~10% of the amount released from the two reservoirs) was stored along 18 river km of the mainstem channel and 25 km of floodplain channels. The Elwha River thus was able to transport most of the released sediment to the river mouth. The geomorphic alterations and changing bed sediment grain size along the Elwha River have important ecological implications, affecting aquatic habitat structure, benthic fauna, salmonid fish spawning and rearing potential, and riparian vegetation. The response of the river to dam removal represents a unique opportunity to observe and quantify fundamental geomorphic processes associated with a massive sediment influx, and also provides important lessons for future river-restoration endeavors.

Published by Elsevier B.V.

1. Introduction

Many fundamental, long-standing problems in earth-surface-process research involve the need to understand how landscapes respond to changing sediment supply (Gilbert, 1917; Antevs, 1952;

Eschner et al., 1983; James, 1989; Benda and Dunne, 1997; Ashworth et al., 2004; Cowie et al., 2008; Covault et al., 2013). Well-controlled laboratory and flume investigations provide valuable steps toward understanding how sediment-supply pulses affect processes such as stream-channel evolution, bar formation, and avulsion (e.g., Lisle et al., 1997; Braudrick et al., 2009; Madej et al., 2009; Tal and Paola, 2010; Pryor et al., 2011); and modeling studies allow simulated manipulation of landscapes over a range of scales (e.g., Cui and Parker, 2005;

* Corresponding author. Tel.: +1 831 460 7533.

E-mail address: aeast@usgs.gov (A.E. East).

Jerolmack and Paola, 2007; Karssenberg and Bridge, 2008; Wang et al., 2011). However, opportunities to study landscape response to major sediment influx over large field scales are much rarer and usually are not anticipated in advance (e.g., dam failure, volcanic eruptions, landslides, or debris flows; Meyer and Martinson, 1989; Montgomery et al., 1999; Hoffman and Gabet, 2007; Casalbore et al., 2011; Gran, 2012; Guthrie et al., 2012; Pierson and Major, 2014; Tullos and Wang, 2014). Therefore, landscape adjustment to a substantial sediment-supply increase remains seldom quantified in the field. In this study we analyze river channel and floodplain response to a uniquely large and anticipated sediment pulse resulting from the largest dam removal globally, on the Elwha River, Washington, USA (Fig. 1).

Conveyance of a large-scale sediment slug, or wave, down a gravel-bed river can evolve through dispersion and translation (Nicholas et al., 1995; Lisle et al., 1997, 2001). Grain-size distribution of the wave, grain size relative to the extant bed, sediment-pulse volume, river discharge, slope, and channel width all influence the speed and evolution of the sediment wave (Lisle et al., 1997, 2001; Cui et al., 2003a,b; Cui and Parker, 2005; Lisle, 2008; Sklar et al., 2009). In steep mountain rivers with Froude numbers greater than about 0.4, sediment waves tend to

be dispersive with little translational behavior (Lisle et al., 1997, 2001; Cui and Parker, 2005; Lisle, 2008), though some translation in mountain river settings has been documented if the pulse grain size is smaller than the preexisting bed, has a narrow grain-size distribution, and has a low height-to-length ratio (Pitlick, 1993; Wohl and Cenderelli, 2000; Sklar et al., 2009). For large sediment pulses released (i.e., eroded and transported) during dam removal projects, Pizzuto (2002) posited that dispersion with little translation would dominate sediment-wave dynamics, but dispersion and translation together have been documented for dam removal projects with smaller sediment releases (Simons and Simons, 1991; Doyle et al., 2002; Stanley et al., 2002; Tullos et al., 2010).

Sediment-wave dynamics along a river system have important implications for geomorphic evolution. For example, alluvial sections of gravel-bed rivers subject to increased bedload and aggradation often respond with channel widening and increased braiding (Leopold and Maddock, 1953; Lyons and Beschta, 1983; Knighton, 1989; Madej and Ozaki, 1996; Miller and Benda, 2000; Lauer et al., 2008; Pierson et al., 2011; Czuba et al., 2012). For natural river systems where new sediment is sourced from the upper watershed or from upstream

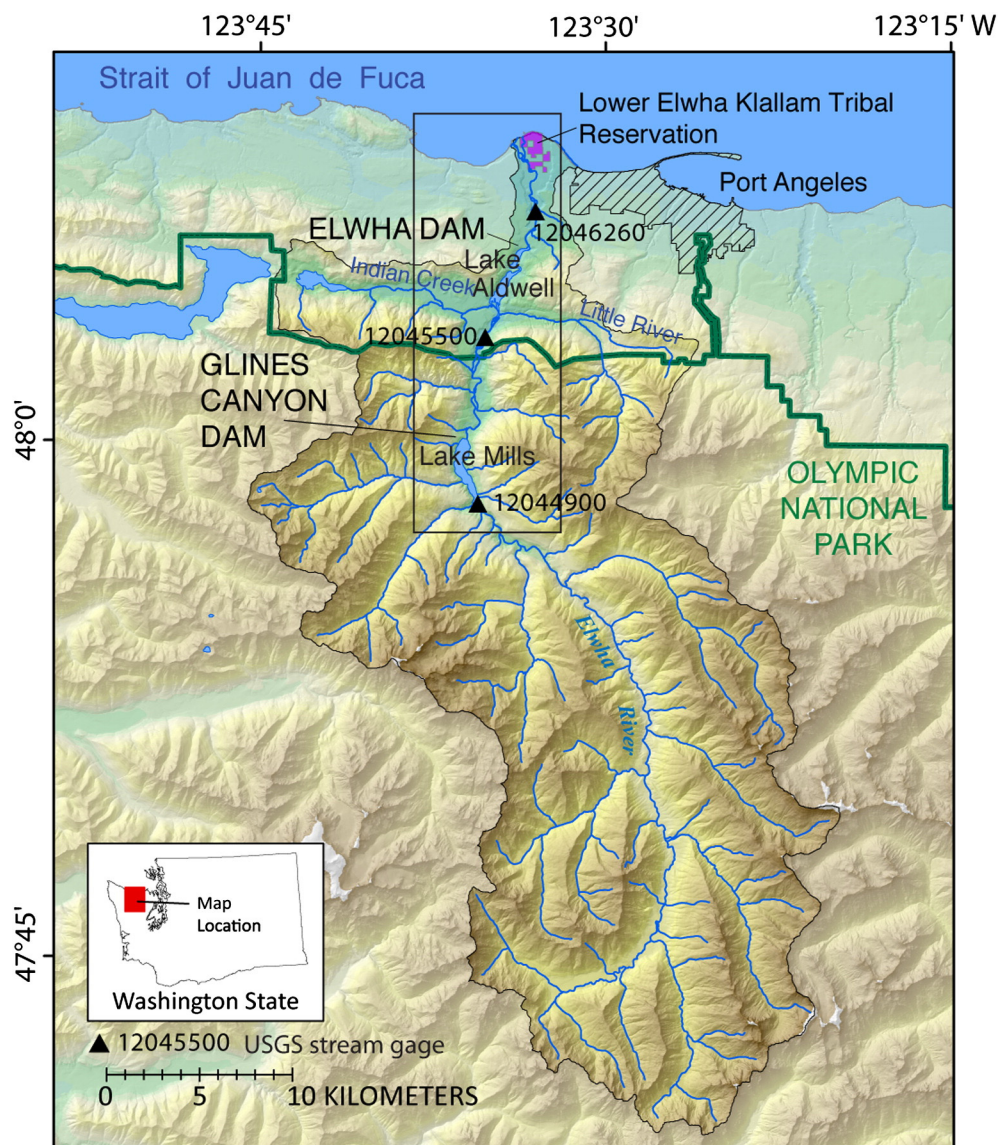


Fig. 1. Elwha River watershed and surroundings, Washington, USA. The Elwha River 'middle reach' extends from Glines Canyon Dam site to the upstream end of former Lake Aldwell; the Elwha River 'lower reach' extends from Elwha Dam site to the river mouth. Box shows location of map in Fig. 3A.

channel migration, increased bedload is usually associated with large flood events. Determining whether channel change is caused by increased bedload or by large floods without increased bedload, or a combination of both, can be challenging (Lyons and Beschta, 1983). The field setting discussed here allows examination of system response to a sediment wave without the compounding influence of large floods.

Sedimentary and geomorphic effects of dams have been discussed thoroughly by others (Williams and Wolman, 1984; Collier et al., 1996; Doyle et al., 2002; Grant et al., 2003; Schmidt and Wilcock, 2008). To review briefly, dams commonly block fluvial sediment transport, and dam operations can alter river flows substantially (Chien, 1985; Dynesius and Nilsson, 1994; Magilligan and Nislow, 2005; Renwick et al., 2005; Syvitski et al., 2005; Grams et al., 2007; Kondolf et al., 2014). Dam operations limit the amount and locations of fine-sediment (sand and finer) deposits downstream from dams (Schmidt and Graf, 1990; Hazel et al., 2006; Dade et al., 2011; Xu et al., 2013). Such altered flow and sediment regimes affect many ecosystem components, altering nutrients and plant, animal, and soil communities (Ligon et al., 1995; Merritt and Cooper, 2000; Vinson, 2001; Shafroth et al., 2002a; Duda et al., 2011; Draut, 2012; Kibler and Tullos, 2013; Zhou et al., 2013).

The ecological effects of dams, as well as the cost of maintaining or upgrading aging structures, have led to dam removal becoming an increasingly common river restoration option, with the recognition that sediment released during dam removal can represent a substantial geomorphic and ecosystem perturbation, at least in the short term (Pizzuto, 2002; Poff and Hart, 2002; Service, 2011). Most of the >1100 dams removed in the United States thus far (American Rivers, 2014) have been <10 m high and impounded modest volumes (<1 million m³) of reservoir sediment (e.g., Cheng and Granata, 2007; Burroughs et al., 2009; Pearson et al., 2011; Sawaske and Freyberg, 2012). Within the past decade, several larger dam removals have provided substantially more information to scientists and managers concerning the physical and biological responses to such events. Notable examples include the removal of the 38-m-high Condit Dam on the White Salmon River, Washington, in 2011, which instantaneously opened a reservoir containing 1.8 million m³ of sediment (Wilcox et al., 2014); removal of the 15-m-high Marmot Dam on the Sandy River, Oregon, in 2007, behind which the reservoir was filled with 0.7 million m³ of sediment (Major et al., 2012); removal of the 12-m-high Savage Rapids Dam on the Rogue River, Oregon, in 2009, which had impounded 0.15 million m³ of sediment (Bounty et al., 2013); and removal of 13-m-high Milltown Dam at the confluence of the Clark Fork and Blackfoot Rivers, Montana, in 2008, which impounded 5.5 million m³ of sediment, almost half of which was mechanically removed to manage contaminated material (Woelfle-Eskine et al., 2012). Dam removal research has also been informed by unintended dam failure events, such as the failure in 2007 of the 38-m-high Barlin Dam, Taiwan, which impounded 10.5 million m³ of sediment (Tullos and Wang, 2014).

The Elwha River dam removal project, involving larger structures and substantially more sediment than in the aforementioned examples (two dams, 64 and 32 m high, impounding ~21 million m³ of sediment), represents an opportunity to study the effects of dam removal and sediment release on a scale not possible in any previous work. We have synthesized data from the first two years of dam removal on the Elwha River to assess fluvial response to substantially increased sediment supply over a two-year interval. Our data demonstrate the dispersion of a large sediment wave and the resulting geomorphic and sedimentary changes in the channel and floodplain along a gravel-bed river. Together with complementary investigations of reservoir-sediment erosion (Randle et al., 2014-in this volume), fluvial sediment transport (Magirl et al., 2014-in this volume), and coastal evolution (Gelfenbaum et al., 2014-in this volume), we characterize a systemwide response that is rare in its scale, yet broadly applicable to other watersheds with major perturbations to sediment supply.

2. Regional setting

The Elwha River flows for 72 km from steep terrain in the Olympic Mountains to the Strait of Juan de Fuca on Washington's Olympic Peninsula (Fig. 1). It drains 833 km², with 83% of the watershed within Olympic National Park, an International Biosphere Reserve and World Heritage site largely managed as wilderness. Steep slopes in the tectonically active basin generate occasional landslides that supply sediment from the upper watershed; glacial outwash alluvium and proglacial lacustrine deposits supply additional sediment in bluffs and terraces along the lower river (Tabor and Cady, 1978; Polenz et al., 2004; Acker et al., 2008). The Elwha River flows through alternating bedrock canyon and alluvial floodplain reaches, the latter having island-braided morphology (cf. Harwood and Brown, 1993; Knighton and Nanson, 1993; Beechie et al., 2006; Warrick et al., 2011). Along much of its length, the mainstem Elwha River is a single, wandering, gravel-bed channel (order B2 of Nanson and Croke, 1992), but in several reaches large bars and vegetated islands separate multiple 'mainstem' threads. The slope of the alluvial sections is 0.4% in the lower reach and ranges from 0.7 to 0.8% in the middle reach between two former dam sites (Fig. 1; we refer to the reach between the dams as the 'middle reach' or 'middle Elwha River' and the reach downstream from Elwha Dam as the 'lower reach' or 'lower Elwha River').

The Elwha River floodplain includes 40 side channels in the middle and lower reaches that are hydrologically connected to the river either through surface flow, groundwater-sourced flow, or (in some places) both. Floodplain channels provide important habitat for juvenile fish and other aquatic organisms (e.g., McHenry and Pess, 2008). The floodplain also contains dense vegetation consisting of shrubs and hardwood and conifer saplings and trees (Kloehn et al., 2008).

Completion of two dams at river kilometer (Rkm) 7.4 in 1913 (Elwha Dam) and at Rkm 21.6 in 1927 (Glines Canyon Dam) substantially changed the physical and biological processes on the Elwha River. Elwha Dam, 32 m high, impounded the Lake Aldwell reservoir to an elevation of 30 m above the pre-dam bed. Glines Canyon Dam was a 64-m-high concrete structure that impounded the Lake Mills reservoir to an elevation of 56 m above the pre-dam bed. The dams were built to supply hydropower to a timber and paper mill operation; neither reservoir provided significant flood control or water supply benefits. The two reservoirs inundated more than 9 km of former riverine habitat, reducing accessible habitat for anadromous salmonid fish by 90% (U.S. Department of Interior, 1996a); Lake Aldwell and Lake Mills also trapped sediment and wood, reduced transport of organic material, and increased downstream water temperatures in late summer and early fall because of heat storage in the reservoirs (Wunderlich et al., 1994). Most dam operations after 1975 were largely run-of-the-river hydrology (Johnson, 1994; U.S. Department of Interior, 1996a); however, there were more rapid daily flow fluctuations and lower daily minimum flows than would have been natural, and occasional autumn releases in dry years to protect native fish populations (Magirl et al., 2011). Annual peak flows on the Elwha River occur from fall and winter storms; secondary peaks of longer duration and smaller magnitude occur from spring snowmelt.

The dams virtually eliminated bed material sediment supply to the river reaches downstream from Glines Canyon Dam (Childers et al., 2000; Curran et al., 2009). The impoundment of 21 million ± 3 million m³ of sediment behind both dams (Randle et al., 2014-in this volume) gradually coarsened the bed sediment downstream, as is common in sediment-supply-limited river reaches downstream from dams (Galay, 1983; Williams and Wolman, 1984; Dietrich et al., 1989), forming an armored bed of predominately cobble grain size (<256 mm; Childers et al., 2000; Pohl, 2004; Draut et al., 2011). The majority of sediment was trapped in the former Lake Mills, behind Glines Canyon Dam (16 million ± 2.4 million m³), where the reservoir sediment was composed of 44% silt- and clay-sized material (<0.063 mm) and 56% coarser sediment. Former Lake Aldwell, behind Elwha Dam,

contained 4.9 million m^3 of sediment and was ~47% silt and clay and 53% coarser sediment (Randle et al., 2014-in this volume). Between one-third and one-half of the sediment in the two reservoirs was projected to move downstream during and after dam removal (Randle et al., 1996; Konrad, 2009), eroded naturally by river flows.

Removal of both dams began on 15 September 2011 (Fig. 2), with the intention to restore the Elwha River ecosystem by allowing unimpeded flow along the mainstem river (see Warrick et al., 2014-in this volume, for summary). The dam removals proceeded in stages timed to minimize negative effects on downstream infrastructure and ecosystem components (Warrick et al., 2012). In this paper we describe changes that occurred over the first two years of dam removal (mid-September 2011 through mid-September 2013), in which Elwha Dam was entirely removed and the height of Glines Canyon Dam was reduced by 75%. We assess the effects of the reservoir sediment release on the downstream river and floodplain system, compare those effects to outcomes that were predicted before dam removal, and consider implications of this and other recent large dam removals for fluvial response to major sediment influx.

From June 2011 to October 2012, Lake Mills and Lake Aldwell were gradually drained of water, with progressive dam-removal notches beginning in September 2011. The gradual, staged removal process drove sediment in the two reservoir deltas to prograde toward the dams. Lake Aldwell was entirely drained of water and coarse-grained sediment was being transported past the former dam site as of mid-March 2012; thereafter, deconstruction continued on the remaining portion of Elwha Dam (which no longer exerted hydraulic control) until removal was completed in September 2012. In October 2012, Lake Mills was entirely drained of water; around 14 October 2012, the reservoir sediment in the former Lake Mills prograded to and overtopped the remaining ~16 m of Glines Canyon Dam, releasing bedload to the middle and lower river. From November 2012 to September 2013, the removal of Glines Canyon Dam was halted because of impacts to a water treatment facility in the lower reach and to allow time for the river to redistribute sediment within the former Lake Mills and along the fluvial channels

downstream from the dams. Glines Canyon Dam removal resumed in October 2013 and was completed in summer 2014.

3. Methods

Characterizing geomorphic response to the Elwha River dam removals required synthesizing data collected by multiple research groups over various spatial and temporal scales. We compiled methods and data from all of these to quantify changes in riverbed and floodplain-channel elevation and topography, bed sediment grain size, and channel planform. From those results, we estimated the sediment mass that accumulated in the mainstem river and floodplain channels over two years of dam removal, forming the fluvial components of a systemwide sediment budget (Warrick et al., 2014-in this volume). In order to distinguish geomorphic change caused by dam removal from natural variability, we compared measurements downstream from the dam sites with those from a control reach upstream from the former Lake Mills and to measurements in many of the same locations prior to dam removal.

3.1. Bed elevation and topographic change detection

We measured bed elevation and topographic change using a combination of temporally continuous water surface elevation monitoring in the mainstem river, which detected topographic changes that affected hydraulic control, and topographic surveys in the mainstem and floodplain channels that measured geomorphic change directly.

3.1.1. Water-surface-elevation monitoring

In sediment-laden rivers, stage of the water-surface elevation can be used as a proxy to detect aggradation or incision of the bed, and thus the evolution of a large-scale sediment wave (Smelser and Schmidt, 1998; Lisle, 2008; Juracek and Fitzpatrick, 2009). Stage does not directly reflect sediment accumulation but reflects the change in hydraulic control immediately downstream from a monitored location and can be used to infer geomorphic change at the hydraulic control. For river sections

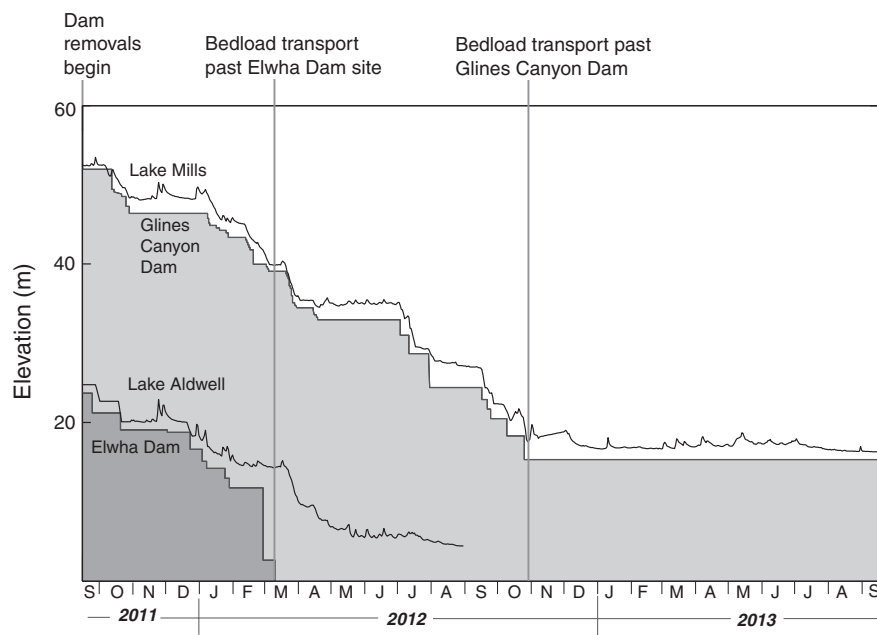


Fig. 2. Changes in water-surface elevations and dam crest heights, relative to original bed elevations, in the first two years of dam removal on the Elwha River, Washington. Glines Canyon Dam (light gray shading) was a 64-m-high concrete structure that impounded its reservoir, Lake Mills, to an elevation of 56 m above the pre-dam bed. Elwha Dam (dark gray shading), 32 m high, impounded the Lake Aldwell reservoir to an elevation of 30 m above the pre-dam bed. Lake elevations were lowered from full pool by 4 m (Lake Mills) and 6 m (Lake Aldwell) between June and September 2011.

with simple hydraulic geometry or linear stage–discharge relations, changes in water-surface elevation for a given discharge provide a reasonable approximation for sediment accumulation or incision at the hydraulic control (Rantz, 1982).

To record stage of the water-surface elevation along the Elwha River, the U.S. Bureau of Reclamation (USBR) and National Park Service (NPS) deployed a stage-gage network of self-recording pressure transducers along the middle and lower reaches in October 2011, with each transducer recording data every 30 min. Stage was also measured at the U.S. Geological Survey (USGS) gaging stations 12046260 (Elwha River at diversion, Rkm 5.1, hereafter ‘diversion gage’; Fig. 1) and 12045500 (Elwha River at McDonald Bridge, Rkm 13.5; hereafter ‘McDonald Bridge gage’). Stage at the diversion gage was measured with a pressure transducer or acoustic Doppler velocimeter, whereas stage at the McDonald Bridge gage was measured with a stilling well, pressure transducer, or noncontact radar sensor as conditions changed (Magirl et al., 2014-in this volume). Stage at the two USGS stations was recorded every 15 min except during instrument failure. The stage instrument at the diversion gage failed for several days in 2012 (24 November, and 30 November to 10 December) as a result of damage from high flow containing abundant sediment and debris.

Hydraulic control at the diversion gage was governed by a concrete broad-crested weir 23 m downstream from the stage sensor. Although sediment accumulated in localized pockets upstream from the weir, observations and instrumentation indicated that little to none accumulated on top of the weir (Magirl et al., 2014-in this volume). Therefore, the stage–discharge relation at the diversion gage remained approximately constant during the study period. By comparing synchronized stage values of the stage-gage network against the stage measured at the diversion gage, we determined the relative change in stage of the stage-gage network. We synchronized discharge between the stage-gage network and the diversion gage by calculating the travel time of flow peaks between gages. By tracking the relative arrival time for dozens of individual peaks (caused by dam deconstruction activities or heavy rainfall) the wave routing celerity was found to be 5.3 and 2.6 km/h in the middle and lower reaches, respectively. The presence of the Lake Aldwell reservoir until April 2012 lengthened the peak-routing time between the middle-river gage (McDonald Bridge gage) and the diversion gage. At the start of dam removal in September 2011 the peak wave routing delay between the McDonald Bridge and diversion gages was 6.8 h, but decreased with the shrinking reservoir in a piecewise linear fashion to about 1.6 h by late April 2012.

The slope of the stage–discharge relation of a gage in the network differed from the stage–discharge relation at the diversion weir. In order to de-trend the stage data from fluctuations in stage owing to variable discharge and to produce a continuous data set of water surface elevations at a given stage gage, differences in the stage–discharge relation between stage gages and the diversion gage were corrected using the ratio of stage between comparison gages from September to December 2011. We assumed that negligible geomorphic change occurred in those first four months of dam removal, a time of modest peak flows and little release of bedload material from either reservoir. This stage–relation ratio allowed adjustment of data from the gage network against the comparative stage measured at the diversion weir for the entire gaging record, thus standardizing the stage–discharge relations between the stage-gage network and the diversion gage. The amplitude of the detected change in water surface elevation may not reflect well the amplitude of sediment accumulation on the river bed, owing to differences in hydraulic control and stage–discharge relation unique to a given stage-gage sensor. Also, the correlation between water surface elevation and bed aggradation is strongest for simple, prismatic channel shapes, and inconsistencies between variables may develop with complex channel topography or complex flow hydraulics. Although the stage-gage network captures general trends in water surface elevation that are broadly indicative of bulk aggradation and can be used to detect sediment wave dispersion, detecting and verifying sediment wave

translation, which depends on precise temporal measurements of bed sedimentation, is more difficult.

We estimated that the stage-gage analysis had an accuracy of about 0.2 m, such that reported stage changes of >0.2 m likely represent significant changes in water surface elevation in the river corridor. This represents a conservative treatment of uncertainty in the stage-gage data; independent measurements by USGS personnel at the McDonald Bridge gage during the study found that reported changes in stage at McDonald Bridge using these methods were within 0.1 m of the actual shifts in the stage–discharge rating.

3.1.2. High-resolution topographic surveys

Within the lower Elwha River, three alluvial subreaches 100–200 m long were targeted for spatially intensive measurements that combined terrestrial lidar (light detection and ranging) scans with total-station surveys. Reaches 1, 2, and 3 (Fig. 3A) were selected to represent a variety of geomorphic conditions and increasing distance downstream from the dams. Reach 1 was 172 m long, centered at Rkm 5.5, and contained six cross sections. Reach 2, 110 m long and containing four cross sections, was within the ‘old mainstem’, an anabranch that received less than half of the river discharge after a large flood in December 2007 altered the mainstem channel configuration slightly. Reach 3 spanned a 112-m-long section centered at Rkm 0.6 and contained six cross sections. An additional control reach, which contained five cross sections centered 1.5 km upstream from Lake Mills, was surveyed to provide a comparison with the downstream areas affected by dam removal. For a detailed discussion of channel evolution in the same subreaches in the five years preceding dam removal, see Draut et al. (2011).

We surveyed these four mainstem subreaches five times between September 2011 (before dam removal) and September 2013, in spring and fall, to resolve changes associated with winter storm floods and spring snowmelt flows. Channel perpendicular cross sections were surveyed using a prism rod and total station. Terrestrial lidar scans were collected in each of those subreaches in September 2011 using a Maptek I-Site 4400 scanner and in September 2013 using a Riegl VZ1000 scanner. The data were filtered using Maptek I-Site software to remove as much vegetation and other objects as possible. Geodetic control for each study reach was established through static differential GPS occupations referenced to the National Geodetic Survey network of continuously operating reference stations (CORS). Positional accuracy of topographic surveys was estimated to be within 2–4 cm. Spatial registration of the terrestrial lidar scanners was accomplished using the same total station and control network used to measure the cross sections, ensuring that the measurements from each instrument were accurately registered to one another. The same survey control network was used in September 2011 and September 2013, ensuring a consistent spatial reference system for each data set.

We also measured geomorphic change in representative examples of the 40 floodplain channels (30 in the middle Elwha River and 10 in the lower river). These channels, which have a combined length of ~25 km, differed hydrologically depending on whether they originated entirely from groundwater, were connected directly via surface water to the mainstem channel, or were groundwater discharge much of the year but had mainstem connection during moderate to high (overbank) flow. Surveys were repeated in eight floodplain channels (four each in the middle and lower reaches) in summer/fall 2010, 2011, 2012, and 2013 and in winter 2011, 2012, and 2013 to assess sediment deposition before and during dam removal.

We used a modified thalweg profile (Mossop and Bradford, 2006) coupled with three cross sections in each of the eight resurveyed floodplain channels to quantify changes in their morphology. Within the thalwegs of floodplain channels, at 40 to 100 survey points that were uniformly spaced unless an obvious elevation change warranted closer spacing, we measured bed elevation, water depth, wetted width, and substrate grain size (Section 3.2), and noted geomorphic settings that characterized habitat type (pool, riffle, or glide). We also measured

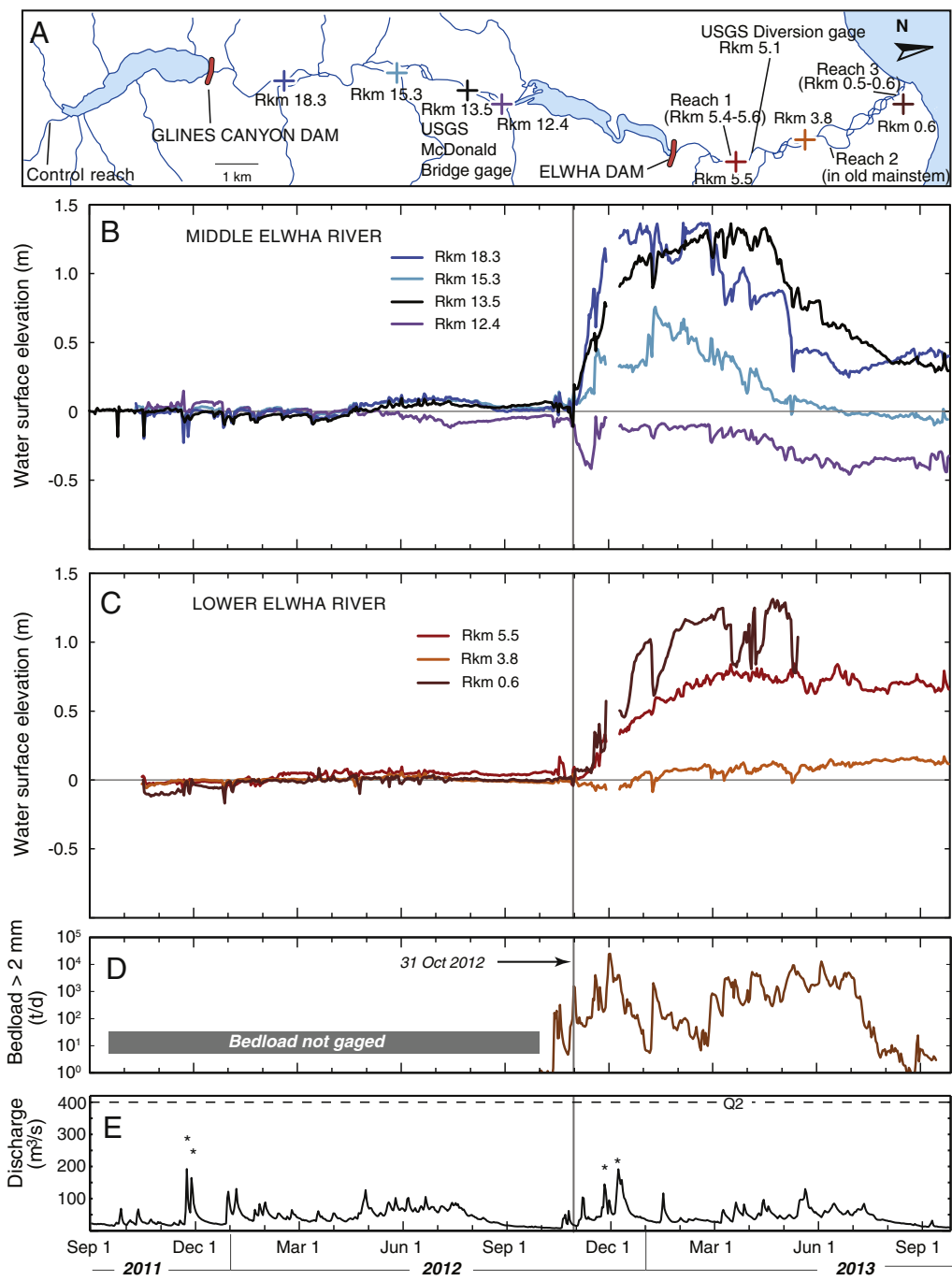


Fig. 3. Water-surface elevation changes during the Elwha River dam removal. (A) Map of Elwha River showing location of stage gages (indicated by colored '+' symbols) measuring water surface elevation. Four other subreaches (control reach above the former Lake Mills, and reaches 1, 2, and 3 within the lower Elwha River) were locations of high-resolution topographic surveys discussed in the text. The 'old mainstem' indicates a 2.6-km-long branch of the lower reach that was the main flow path prior to a large flood in December 2007. (B) Middle reach water surface elevation at Rkm 18.3, 15.3, 13.5, and 12.4. (C) Lower-reach water-surface elevation at Rkm 5.5, 3.8, and 0.6. (D) Bedload (> 2 mm) measured at Rkm 5.1 (Magirl et al., 2014—in this volume). (E) Hydrograph, measured at the USGS gaging station 12045500 (Rkm 13.5). Dashed line shows 2-year peak flow (Q2, 399 m³/s) calculated from a log Pearson type III flood frequency analysis using discharge data from 1897 to 2013, with low outliers removed using the Multiple Grubbs–Beck test. Discharge curve is plotted as daily average values; asterisks show instantaneous peak discharge for the four highest flow events during the study interval.

bed elevation, wetted width, and grain size at three channel cross sections located at the upstream end, middle, and downstream end of each surveyed floodplain channel.

New sediment thickness in the eight repeatedly sampled floodplain channels was measured along the thalweg profile using a 2.54-cm steel rod hammered through the newly deposited sediment to the pre-dam-removal bed. In addition to in-channel measurement of sediment thickness, we also used benchmarks along the floodplain channels to measure changes in streambed elevation of the floodplain channels.

These measurements had an average observation error of <15%, which we calculated from a simulation study to estimate the impact of observation error on the derived metrics. We first estimated the distribution of observation errors in angle measurements used to estimate vertical distance from one point to the next. We assumed that the measurements were unbiased and normally distributed. The standard deviation of measurements was estimated to be 0.5°. Using this error we then simulated the same profile 1000 times with errors generated from the observation error distribution (normal with mean of 0 and s.d. of

0.5). We then examined the resulting distributions of profile statistics (described above) to assess their sensitivity to measurement error. These observation error simulations revealed that thalweg profile measurements had a coefficient of variation (CV) of <15% for several metrics, including channel gradient, the proportion of pools, the maximum depth of the floodplain channel, the mean maximum depth, and the mean square error. Therefore, we assumed that the relative bed elevations measured during the floodplain channel surveys also had a CV of <15%.

3.1.3. Longitudinal profiles

We measured longitudinal profiles of the Elwha River mainstem channel bed and water surface elevation along the middle and lower reaches prior to the start of dam removal in early September 2011 and again during dam removal in July 2012, November 2012, and May 2013. Profile data were collected by boat with a mounted acoustic Doppler current profiler (ADCP) or single-beam depth sounder combined with survey-grade GPS equipment to measure water surface elevation. The water stage data were collected in rapid mode, i.e., storing one observation every 1 to 2 m along the path of the boat. In the September 2011 survey before dam removal, we completed multiple boat passes across the channel at numerous locations to ensure that the longitudinal profile followed the thalweg. In the surveys during dam removal, boat paths generally followed the new, shallower channel thalweg during each survey; channel margins during dam removal were too shallow to measure with depth-sounding equipment. We combined depth data with water surface elevation data to compute channel bed elevations. Depth and water surface elevation data were then projected to the closest point along a common channel centerline for all surveys (using ArcGIS) to generate longitudinal profiles. Longitudinal profile data had a vertical accuracy of ± 0.2 m based on survey equipment specifications and as much as ± 0.3 m when accounting for water turbulence and substrate variability along the channel bed.

3.2. Bed sediment grain size

Comparing bed sediment grain size before and during dam removal is a crucial component of analyzing both the physical changes and potential ecological effects of the Elwha River restoration. Prior to dam removal, we used pebble counts (cf. Wolman, 1954) to document bed sediment grain size of riffle crests and subaerially exposed bars along the active channel throughout the middle and lower reaches (U.S. Department of Interior, 1996a). After dam removal began, we collected pebble counts and bulk samples on recently active (subaerially exposed, unvegetated) sediment bars. Pebble counts, which were used up until September 2012 (prior to major bedload release from the former Lake Mills reservoir), used a standard 100-count method along channel-perpendicular transects; size classes were recorded using a gravelometer. Beginning in November 2012, after bedload release had made riverbed sediment too fine for pebble counts to be feasible in many places, bulk sediment samples were collected and analyzed instead. Each bulk sample included ~38 L of sediment from a 1-m \times 1-m square, extracted from the uppermost 10 cm of substrate using a trowel. Sediment 16 mm and coarser was sieved in the field, and sediment finer than 16 mm was dried and sieved down to 0.062 mm at the Analytical Resources, Inc., laboratory in Seattle, WA. Resampling of extant ripple crests after dam removal had not been repeated as of this writing, owing to burial of former ripple crests and flows not having been low enough to allow extensive thalweg sampling.

Within the four mainstem subreaches (reaches 1–3 in the lower Elwha River and the control reach above the former Lake Mills), bed sediment grain size was measured using the CobbleCam technique of Warrick et al. (2009). This method uses an autocorrelation algorithm of pixels in digital photographs (Rubin, 2004) to calculate mean grain size of sediment ranging from medium sand to boulders and is accurate to within ~14% for grain sizes up to 200 mm in natural field lighting (Warrick et al., 2009). Downward-looking photographs were taken of

subaerially exposed, unvegetated sediment at locations that included the survey cross sections (Section 3.1.2) and, after dam removal began, along additional, representative transects across any new sediment deposits that did not fall on a survey cross section. For sediment finer than medium sand, we measured grain size using a Coulter laser particle size analyzer at the U.S. Geological Survey sediment laboratory in Santa Cruz, CA, after having removed organic matter with a hydrogen peroxide solution.

Within the eight floodplain channels measured, we conducted pebble counts using a standard 100-count method (cf. Wolman, 1954) along each of the three channel cross sections.

3.3. Channel planform analysis

To assess the effect of increased sediment supply on channel planform, we analyzed the mainstem sinuosity and degree of channel braiding evident in aerial imagery. Aerial composite, pixel-averaged orthoimages were generated from multiple overflights with a fixed-wing plane operated by the National Park Service during dam removal. The orthoimages used overlapping digital photographs containing ground control points of known location and elevation to obtain high-resolution topography using Structure-from-Motion (SfM), a technique developed for computer vision (Snavely et al., 2008; Westoby et al., 2012; Javernick et al., 2014; Randle et al., 2014-in this volume). Channel sinuosity and braiding index were determined for four sets of aerial images taken during low flow—one from 25 August 2011, shortly before dam removal began, at a river discharge of 34 m³/s, and three sets taken during dam removal: 10 August 2012 (29 m³/s), 13 February 2013 (35 m³/s), and 19 September 2013 (9 m³/s).

We delineated bank lines and sediment bars on the orthoimages using ArcGIS and digitized them at a scale of 1:500. Channel center lines were derived by computing polygons on the vertices of the bank lines, then removing polygon edges intersecting the channel margins and removing dangling nodes. Downvalley distance was measured as a straight line from the beginning to the end point of the channel centerline, considering the middle and lower reaches separately. Mainstem sinuosity was calculated as the length of the channel carrying the most water, divided by downvalley distance. We quantified channel braiding index in terms of total channel length, calculating the sum of mid-channel lengths of all channels divided by the length of the mainstem centerline (Friend and Sinha, 1993). This method evaluates a slightly different braiding characteristic than those based on the total number of channels (Howard et al., 1970; Egozi and Ashmore, 2008) but provides results that are fundamentally the same (Draut et al., 2011).

3.4. Sediment accumulation estimates

We used the topographic, sedimentary, and channel planform measurements together to estimate the sediment mass accumulation in the Elwha channel and floodplain after the first two years of dam removal. We used two methods to estimate accumulation in the mainstem river and three methods to estimate accumulation in the floodplain channels.

To estimate the sediment accumulation in the mainstem channel as of September 2013, our two methods, M1 and M2 (mainstem 1 and mainstem 2), were based on separate data sets that covered different portions of the river corridor at variable spatial and temporal scales. For the eventual mass-balance calculations (Section 4, and Warrick et al., 2014-in this volume) we relied on M2 because of its greater spatial coverage after having verified its accuracy by comparison with the results of M1 in the lower river.

Method M1, which applied only to the lower river, was based on volume change measured from the combined high-resolution total-station and terrestrial lidar surveys in the four subreaches (Section 3.1.3) in September 2011 and September 2013. Because terrestrial lidar scans detect subaerially exposed surfaces but cannot resolve the subaqueous

riverbed, the elevation differences in subaqueous areas of the four subbreaches were measured using the cross sections surveyed with a rod and total station contemporaneously with lidar data collection. To calculate volumetric change in each subreach over those two years, we generated triangulated irregular network (TIN) surfaces of each data set by merging the subaqueous total-station cross sections with the subaerial lidar data. Break lines were manually inserted along banks, parallel to, and between subaqueous total-station transects to minimize across-channel interpolation errors. These break lines ensured that each TIN was faithful to the total-station measurements for the subaqueous regions and faithful to the lidar data for the subaerial regions.

To calculate volumetric change, each TIN was converted to a gridded surface with a 0.1-m cell size. Digital elevation models (DEMs) of difference (DoD) were created by differencing the 2013 DEMs from the 2011 DEMs. Elevation changes below the reliable level of detection (LoD) for each surface were removed, or thresholded, based on techniques outlined by Brasington et al. (2003), Lane et al. (2003), and Wheaton et al. (2010). To calculate the LoD values used for thresholding, elevation uncertainties for each DEM were estimated by comparing individual grid-cell elevations to independent contemporaneous total-station measurements. The standard deviation of the elevation (SDE) residuals between these total-station check data and the DEM was used to estimate a uniform elevation uncertainty for the entire surface. The DEM elevation uncertainties were summed in quadrature to calculate a minimum LoD for the elevation changes between September 2011 and September 2013. The LoD was used to remove all elevation changes below the 95% confidence limit for reliable detection. The remaining elevation changes were used to calculate net volume change.

To estimate uncertainty in the net volume calculations, we estimated unsystematic and systematic errors using the independent total-station check data. Unsystematic errors were estimated using the SDE and propagated through the volume calculations using the method of Lane et al. (2003). Systematic error was estimated using the mean bias error (MBE) of the residuals between the independent total-station measurements and each DEM. These were summed and multiplied by each subreach analysis area to estimate a total volume uncertainty for each LoD. The MBE of the total-station check data residuals likely overestimates the measurement uncertainty; total-station measurements and terrestrial lidar measurements tend to measure different elevations in a given local surface if the substrate is coarse-grained, as was the case before dam removal in September 2011. Total-station measurements rely on a prism rod being placed on the ground, often preferentially between large sediment clasts (e.g., cobbles) instead of on top of them. Terrestrial lidar measurements optically record the top surfaces of large clasts and, to a lesser degree, slightly lower elevations between clasts. Thus each measurement technique tends to be biased toward different elevations of the same local surface, and the MBE between the two is partly a function of surface roughness or grain size. Even with very high instrument precision, a comparison of measurements recorded from each system would likely reveal some vertical bias that would not be indicative of true measurement uncertainty. A significant portion of the systematic volume uncertainty calculated using this technique likely results from these differences in the measurement techniques; however, these sources of MBE remained small enough (<0.05 m vertical error) that a clear signal was ultimately detected (Section 4.4).

The sediment volume difference for each subreach was converted to mass assuming a dry bulk density range of 1200–1700 kg/m³. The low end of this range (1200 kg/m³) represents the mean of dry bulk density values that we measured in 13 samples of post-dam-removal sediment collected from channel margin bars in the mainstem river in March 2013 and analyzed in the Santa Cruz USGS laboratory. At that time it was not feasible to sample the new mid-channel bars, which were largely submerged and unstable; however, grain size analysis of their surface sediment later in 2013 revealed that granule and pebble sizes were dominant (discussed below). Therefore, our March 2013 bulk density analyses were assumed to be biased toward the finer grain

sizes present. To more fully represent the likely density range in the new deposits, we used 1700 kg/m³ as a suitable end-member value for poorly sorted coarse sediment (sand, gravel, and cobbles; Geiger, 1963), which was also representative of the mean bulk density in the Elwha reservoir sediment (Wing, 2014).

The inferred mass accumulation in reach 1, the subreach with channel dimensions and morphology considered most representative of the lower river in general, was divided by the subreach length (172 m) to yield a mass per unit river length. Extrapolating this mass per unit river length along 6.6 km of the lower river yielded a value for new sediment mass in the lower Elwha River mainstem. Added to that was an estimate calculated similarly for reach 2; the inferred mass per unit river length accumulating in reach 2 was extrapolated along the 2.6-km-long old mainstem channel. Finally, for the lowermost 0.3 km of the lower river, downstream from the last riffle, we calculated the new sediment mass based on similarly combined lidar and cross section survey data from reach 3. We used a separate extrapolation for that lowermost portion of the river because reach 3 was (and is) geomorphically unconfined, contained an exceptionally large pool in 2011, and experienced backwater effects where the river meets the Strait of Juan de Fuca, all of which contributed to that subreach accumulating an exceptionally large amount of sediment per unit river length. Volumetric change in the lower river was also compared against that measured in the control reach, upstream from the former Lake Mills, where surface change between September 2011 and September 2013 was analyzed using the same procedure just described.

A second method, M2 (mainstem 2), was used to estimate sediment accumulation in the middle reach, where high-resolution terrestrial lidar and total-station survey data were not available, and in the lower reach, where its accuracy was appraised by comparing its results with those of method M1. In method M2 we calculated sediment accumulation in the mainstem channel as of September 2013 based on computed volume change for the entire length of the middle and lower river reaches from differences between pre- and post-dam-removal DEMs covering the unvegetated (recently active) channel area. We developed a DEM suitable for representing the pre-removal middle and lower mainstem Elwha River by combining subaerial topographic data from an April 2012 aerial lidar survey with bathymetric data collected from boat-mounted ADCP bathymetric surveys in summer 2011. We used the April 2012 aerial lidar data because, although those data were collected after the start of dam removal, they preceded the major release of bedload sediment from either reservoir and so preceded substantial geomorphic change, as we show below (Section 4). In an approach similar to method M1, in method M2 we separated lidar and ADCP measurements with a break line inserted at the water edge of the lidar data. In a few areas of the river that were inaccessible by boat in summer 2011 or had poor GPS coverage, we estimated depths for the wetted channel based on measured water surface elevations minus depth values based on channel bottom measurements from earlier surveys (U.S. Department of Interior, 1996a). Depth estimates were informed by aerial lidar data and by measured values over comparable geomorphic features. Channel bed elevations were then interpolated using a spline algorithm and the ADCP data with the shoreline as the break line. The lidar and interpolated bathymetry then were used to construct a TIN and generate a DEM.

Post-dam-removal elevations were partitioned into subaerial and subaqueous components by digitizing bank lines and bars from 19 September 2013 orthoimagery, as described in Section 3.3. Subaerial deposition as of September 2013 was calculated by differencing elevations measured from the 19 September 2013 SfM-derived DEM from the pre-dam-removal DEM to create a DoD for subaerial surfaces. New sediment thickness below the water surface was calculated by generating a top-of-sediment DEM based on channel bottom profiles surveyed with ADCP or single-beam sonar on 30 July and 1 August 2013 in the middle and lower river, and subtracting the pre-dam-removal DEM to create a DoD for the subaqueous regions. Because the

water was turbid during those summer 2013 channel bottom surveys, we verified depth data by manual probing throughout the bathymetric data collection. For the first 1.5 Rkm downstream from each dam site, the subaqueous portion of the new sediment volume was estimated by assuming that the pre-dam-removal pools had filled with sediment, based on aerial photographic and direct field observations. Values from the subaerial and subaqueous DoDs were summed to calculate total sediment storage volume in the middle and lower reaches.

We estimated uncertainty for each DoD generated using method M2 by assuming that the vertical error of the pre- and post-dam-removal DEMs was normally distributed (Taylor, 1997; Lane et al., 2003). Uncertainty was computed separately for the subaerial and bathymetric DoDs. Bathymetric vertical uncertainty was calculated by summing in quadrature the estimated vertical errors associated with equipment specifications and boat movement. A thorough review and post-processing of bathymetric data were assumed to have removed systematic errors. A constant vertical error multiplier was then added to account for areas where data had to be extrapolated to develop a continuous 3-m² DEM. Subaerial vertical uncertainty was calculated using the standard deviation of checkpoint measurements for airborne lidar and SfM DEMs (Lane et al., 2003). Following error propagation principles (Taylor, 1997), uncertainty for each DoD was then calculated using the method of Lane et al. (2003). Assuming independent, random error, where two surfaces with a concurrent regular grid-cell size are differenced, the volumetric uncertainty can be derived by integrating the uncertainty of each grid cell (Eq. 15 of Lane et al., 2003). We applied this uncertainty-propagation method using the larger grid-cell size of the pre-removal DEM for the subaerial and subaqueous DoDs. Uncertainty for each DoD was then summed, rather than summed in quadrature, because both post-removal DoDs relied on the same pre-removal DEM and therefore could not be considered independent and because each DoD represented a separate portion of the analysis area. The actual uncertainty likely varies spatially owing to topographic complexity, GPS dilution of precision, water turbulence, and SfM ground control. These additional sources of error, which are difficult to quantify, are the subject of active research (Wheaton et al., 2010; Milan et al., 2011). Finally, to convert sediment volume to mass, we assumed a dry bulk density range of 1200–1700 kg/m³.

We used our floodplain surveys (Section 3.1.2) to estimate the total new sediment volume in floodplain channels using three different methods. Our techniques for volume change estimation in floodplain channels differed from those in the mainstem river because the abundant floodplain vegetation greatly complicates DEM generation from either airborne or ground-based remote-sensing data. Floodplain method 1 (F1) assumed the same average new sediment depth (0.41 m) in each of the floodplain channels in the middle and lower reaches. The average sediment depth was based on the average accumulation depth measured in the eight floodplain channels during dam removal (Section 4). Method F1 also assumed no change in channel dimensions from pre-dam-removal hydraulic geometry and simple filling of a floodplain channel. We then calculated the estimated sediment volume for all eight floodplain channels measured and compared that to the actual accumulation depths and widths measured to generate a correction factor that could be applied to the 32 floodplain channels not measured (correction factor = 1.06). Hence, sediment accumulation using method F1 was estimated as channel area × 0.41 × 1.06.

Floodplain method 2 (F2) used a combination of the cross sections and thalweg profile to estimate the amount of sediment accumulation in the floodplain channels. First we calculated the area of sediment that accumulated at each cross section ($xsArea_j$) using the cross section data from each of the eight floodplain channels remeasured (Eq. (1)):

$$xsArea_j = \sum_{i=1}^n \frac{(xsDist_{i+1} - xsDist_i)(xsSedDepth_i + xsSedDepth_{i+1})}{2} \quad (1)$$

where j is the number of the individual cross section, incremental values of i represent consecutive surveyed points in the cross-channel

direction, and n is the total number of surveyed points in each cross section. These areas were then standardized by dividing by the sediment depth at the cross section point with the lowest elevation (approximate location of the thalweg, $xsSedDepth$):

$$xsAreaStnd_j = \frac{xsArea_j}{xsSedDepth_{\min(elevation)}}. \quad (2)$$

For each segment of the thalweg profile, the volume of new sediment ($segVol_i$) was estimated as the segment length times the average of the nearest two cross section areas, which defined the start and end points of the thalweg segment (Eq. 3):

$$segVol_i = (thDist_{i+1} - thDist_i) * \frac{xsAreaStnd_a * thSedDepth_i + xsAreaStnd_b * thSedDepth_{i+1}}{2} \quad (3)$$

where a and b represent the cross sections assigned to thalweg points (i) and ($i + 1$), respectively; $thDist_i$ and $thDist_{i+1}$ represent the distance from the first survey point (1) to (i) and ($i + 1$) survey points, respectively. The two areas (of new sediment at the start and end points of each thalweg segment) were scaled to the thalweg points by multiplying the assigned standardized cross section area ($xsAreaStnd_j$) by the depth of new sediment at those points measured in the thalweg profile ($thSedDepth_i$). We then summed the volumes of each segment in the thalweg profile to estimate the total sediment volume for the thalweg profile ($totVol$):

$$totVol = \sum_{i=1}^n (segVol_i). \quad (4)$$

Finally, we compared the estimated $totVol$ to the estimated amount for all eight floodplain channels measured, and calculated a correction factor that could be applied to the sum of all 32 floodplain channels not measured. The correction factor for method F2 was 1.64.

Floodplain method 3 (F3) was a hybrid of F1 and F2. As in F1 we assumed the same average sediment depth (0.41 m) in each of the floodplain channels in the middle and lower reaches, except that we estimated sediment accumulation separately for each of the eight channels measured rather than for the aggregate area of all eight channels as in F1. Method F3 also assumed no change in channel dimensions from pre-dam-removal hydraulic geometry and a simple filling of a floodplain channel. We then calculated the estimated amount for all eight floodplain channels measured and compared that to the actual amount measured to come up with a correction factor that could be applied to the sum of all 32 floodplain channels not measured. The correction factor for method F3 was 2.44. Notably, each of the methods necessitated using rather substantial correction factors, a result of sediment having accumulated in spatially nonuniform patterns.

After obtaining volume estimates for floodplain channels using methods F1, F2, and F3, we converted the volumes to mass assuming a dry bulk density range of 1200–1700 kg/m³. We assumed that deposition on the floodplain outside of floodplain channels was negligible between September 2011 and September 2013. Although several floodplain locations accumulated new sediment in some areas outside of channels (Draut and Ritchie, 2013; P.B. Shafroth, unpublished data), these deposits were small, discontinuous patches, as river flows had not been high enough to deposit sediment over a substantial area outside of the floodplain channels.

4. Results

A large influx of sediment from the two former reservoirs (Curran et al., 2013; Magirl et al., 2014-in this volume; Randle et al., 2014-in this volume) substantially affected the Elwha River morphology and sediment composition in the first two years of dam removal. During

that time ~6 million m³ of reservoir sediment (9.1 million t) were released from the former Lake Mills and 1.1 million m³ (1.4 million t) were released from former Lake Aldwell (Randle et al., 2014-in this volume), totaling 7.1 million m³ (10.5 million t) and representing ~37% and ~23% of the total stored sediment in the Mills and Aldwell reservoirs, respectively. Given that the natural annual sediment load would have been 217,000–513,000 t (Curran et al., 2009; Czuba et al., 2011), this reservoir sediment release represented several decades' worth of stored sediment.

Sediment accumulation downstream from both dam sites was evident in all of our measurements of topography, sediment composition, and channel planform. We are confident that the new sediment in the middle and lower Elwha River was supplied from the two former reservoirs, rather than being a natural supply increase from the upper watershed (e.g., from a landslide that could have been undetected in such a remote wilderness setting), because the control reach upstream from

the former Lake Mills remained unchanged (discussed below). Moreover, estimated bedload into the former Lake Mills from the upstream watershed, based on established sediment-rating curves (Curran et al., 2009), was a modest 8000 t from September 2011 to September 2013 (Magirl et al., 2014-in this volume). Notably, the observed changes occurred without the river having approached flood stage between September 2011 and September 2013. The highest discharge on the Elwha River within those two years was 291 m³/s on 23 November 2011, representing 73% of a 2-year peak flow event.

4.1. Bed elevation and topographic change

Stage-gage measurements (Fig. 3A–C) showed changes in water-surface elevation that were broadly indicative of changes in riverbed elevation. Water-surface elevations provided a record at high temporal resolution that complemented the bed-elevation changes measured

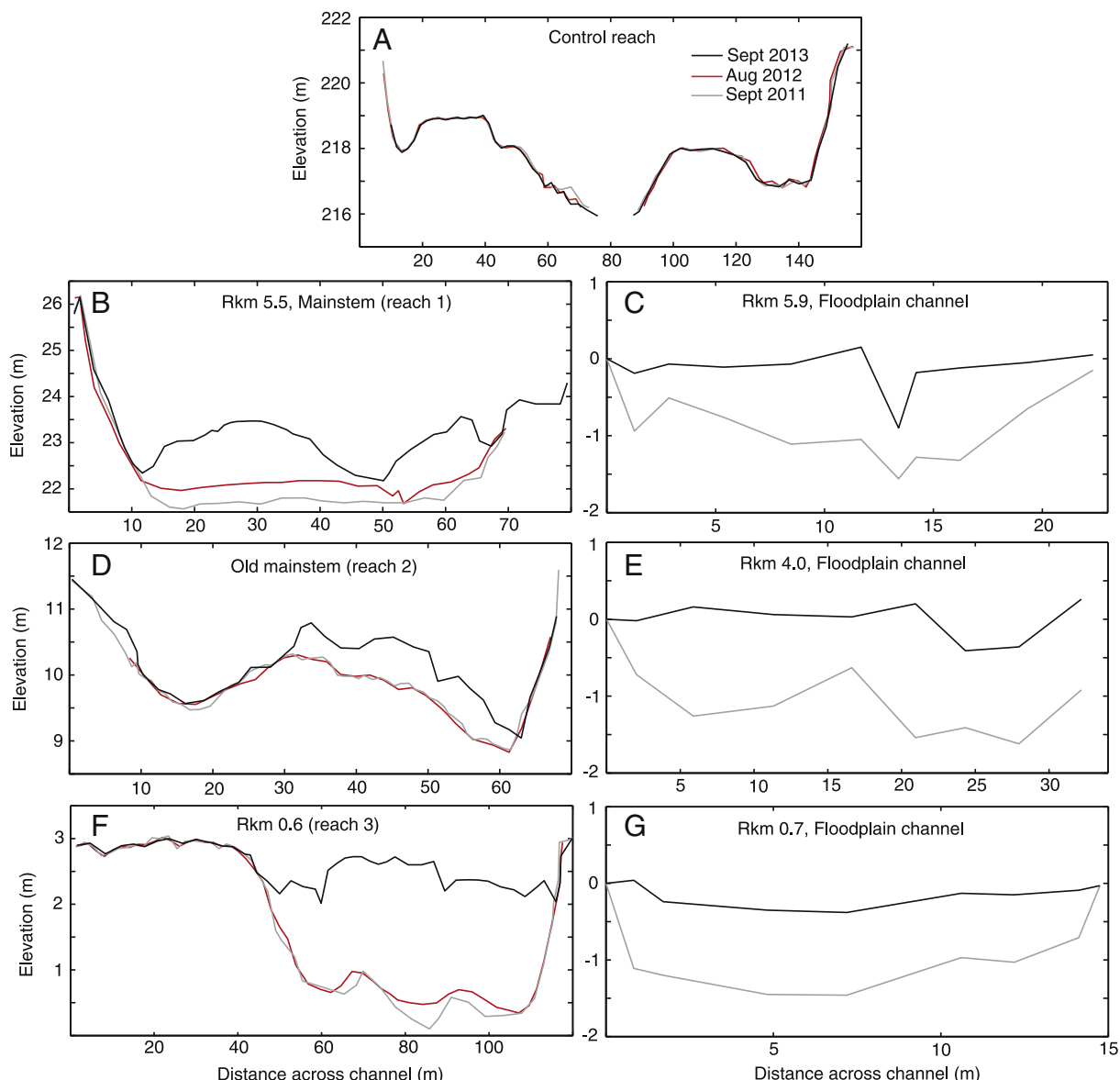


Fig. 4. Examples of topographic change on channel-perpendicular transects in the mainstem Elwha River and floodplain channels. Gray, red, and black lines show bed elevation in September 2011 (before dam removal), August 2012, and September 2013, respectively. Locations are as shown in Fig. 3A. (A) One of five transects in the control reach, upstream from the former Lake Mills, unaffected by dams or their removal. (B) Transect at Rkm 5.5, one of six transects in reach 1. (C) Transect across a floodplain channel near the mainstem location in (B), corresponding to Rkm 5.9. (D) One of four transects within the 2.6-km-long old mainstem anabranch (reach 2), lower river reach. (E) Transect across a floodplain channel near the location in (D), corresponding to Rkm 4.0. (F) Transect at Rkm 0.6, one of six transects within reach 3. (G) Transect across a floodplain channel near the location in (F), corresponding to Rkm 0.7. The same mainstem transects in A, B, D, and F were also surveyed in April 2012 and March 2013 (data not shown, for clarity). Elevations of mainstem profiles (A, B, D, F) are given relative to NAVD88 datum. Elevations of floodplain profiles (C, E, G) are given relative to elevation at the stream-left edge of each channel as measured in the initial survey.

directly in the less frequent but higher spatial resolution topographic surveys (Figs. 4, 5, and 6). Water-surface-elevation changes through the middle and lower reaches corresponded temporally with elevated bedload (Fig. 3D). Hence, we compared daily bedload >2 mm measured at the diversion gage to changes in bed and water-surface elevation (Fig. 3D; data from Magirl et al., 2014-in this volume); we assumed strong correspondence between bedload (sand and gravel) and detectable topographic change. Bedload was not measured from September 2011 to September 2012, but analysis by Magirl et al. (2014-in this volume) indicated that bedload at the diversion gage over that first year of the study was about an order of magnitude less than bedload in the second year (September 2012–September 2013).

In the first year of dam removal, the modest flow regime (no flows approaching the two-year flood) coupled with a load of only suspended sediment passing Glines Canyon Dam did not affect water-surface elevation measurably in the middle reach (Fig. 3B). The stage gages at Rkm 18.3, Rkm 15.3, and Rkm 13.5 showed changes in water surface elevation of <0.1 m through the first year (Fig. 3B). An apparent slight stage increase in middle-reach gages between May 2012 and August 2012 reflected differences in the stage-discharge relation that were not fully corrected; the apparent aggradation then was likely an analysis artifact (Fig. 3B). The stage gage at Rkm 12.4 was positioned in the headwaters of the former Lake Aldwell sediment delta. Our data showed a small decrease in water-surface elevation at Rkm 12.4 in 2012, which reflected incipient incision of the river into Lake Aldwell reservoir sediment in response to lowered base level. However, that water-surface elevation decrease at Rkm 12.4 was on the same order of magnitude as our observation uncertainty.

Changes in water-surface elevation in the lower Elwha River during the first year of dam removal were of a similar magnitude to those in the middle reach (Fig. 3C), despite the fact that bedload derived from the former Lake Aldwell reservoir deposit was passing the Elwha Dam site

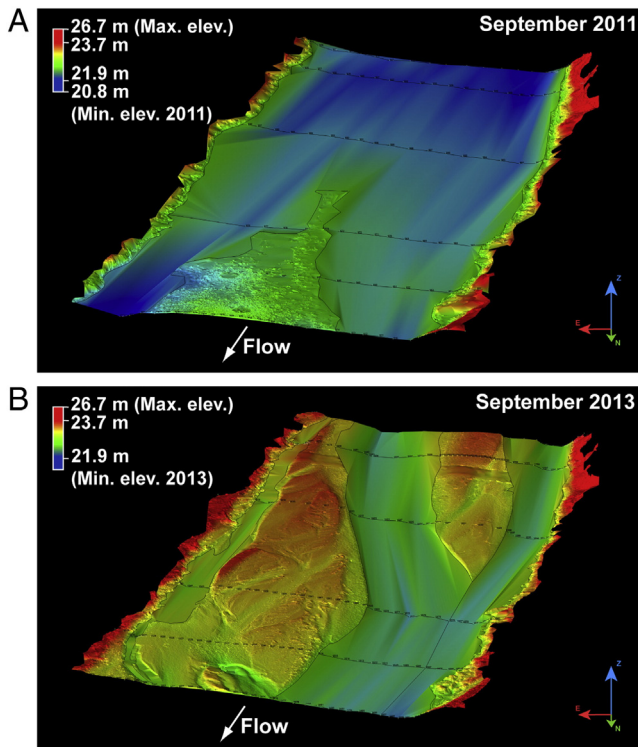


Fig. 5. Example of topographic change measured by combining terrestrial lidar scans and total-station surveys. Images show topographic change in reach 1, spanning Rkm 5.4–5.6 in the lower Elwha River, between (A) September 2011 and (B) September 2013. New sediment deposition during dam removal is apparent as bed aggradation and new bar formation. Width of TIN surface at the foreground (downstream end) of each image is ~90 m. Elevations are given relative to NAVD88 datum.

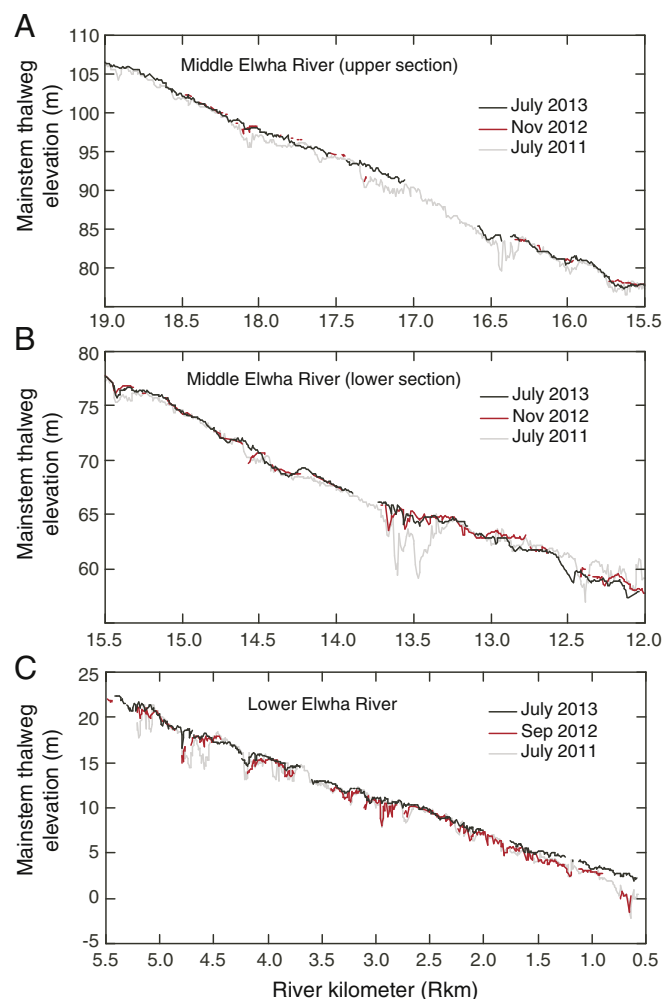


Fig. 6. Longitudinal profiles of the Elwha River. Each plot shows thalweg bed elevation from a pre-dam-removal survey (gray), and subsequent profiles surveyed during dam removal (red and black). (A) Profile of the middle reach from Rkm 19.0 to Rkm 15.5. (B) Profile of the middle reach from Rkm 15.5 to Rkm 12.0. (C) Profile of the lower reach from Rkm 5.5 to Rkm 0.5. Elevations are given relative to NAVD88 datum.

by April 2012 (Magirl et al., 2014-in this volume). Stage gages at Rkm 5.5, 3.8, and 0.6 through September 2012 all recorded changes in water surface elevation of $<\pm 0.1$ m. This is broadly consistent with direct bed measurements in the lower reach, where aggradation on the order of 0.1 m was typical as of spring and summer 2012, largely in the form of sand and mud having deposited in interstitial spaces within the pre-dam-removal cobble bed (Draut and Ritchie, 2013). Some new sand and gravel deposits with a maximum thickness of 0.5 m were measured in the lower river in late summer 2012 (Fig. 4); this was consistent with local deposition measured in longitudinal profiles, though sediment thickness was locally greater where pools filled (Fig. 6C). In the lower reach large, low-velocity pools (i.e., pools ~100 m long and 3 m deep; Rkm 5.5 to 3.75) filled with new coarse sediment released from former Lake Aldwell between April and September 2012, whereas smaller, higher-velocity pools downstream from Rkm 3.5 were less affected (Fig. 6C). Pool filling in the lower reach in the first year of dam removal evidently did not represent enough sediment deposition to affect water-surface elevations significantly (Fig. 3C).

During the first year of dam removal new sediment also accumulated in the floodplain channels of the lower reach and to a much lesser extent in those of the middle reach. Average new sediment thickness in the measured floodplain channels of the lower reach was 0.39 m (± 0.43 m), whereas the middle reach floodplain channels had an average new sediment accumulation of 0.02 m (± 0.01 m). Most sediment

that accumulated in floodplain channels in the middle and lower reaches was sand-sized or finer and was deposited in the lee of obstructions (e.g., logjams) and in deep pools. Sediment deposition did not extend throughout the floodplain channels but occurred in discrete sections associated with the obstructions.

In the second year of dam removal, the riverbed aggraded substantially throughout the middle and lower reaches. In middle to late October 2012, sand and gravel (>2 mm) derived from the former Lake Mills began spilling over the lowered Glines Canyon Dam and a series of storms increased overall sediment load (Fig. 3D; Magirl et al., 2014-in this volume). Detectable bedload in the lower river at the diversion gage, on the order of 100 t/d, started on 14 October 2012 and ranged from 10 to 100 t/d through the end of October. A heavy rain event on 31 October 2012 resulted in a peak flow of about 150 m³/s, and multiple days of bedload as great as 1000 t/d carried downstream from the former Lake Mills (Fig. 3D). In the middle reach all gages in the stage-gage network responded to the sediment pulse within a week of the 31 October 2012 rain event with aggradation or incision (Fig. 3B). All the stage gages except that at Rkm 12.4 showed aggradation of +0.5 to +1.5 m at that time. By mid-November 2012 the longitudinal profile showed accumulation throughout the middle reach, particularly in large pools (i.e., Rkm 14.0 to 13.3; Fig. 6B). We also observed aggradation between riffle crests then, consistent with measurements of increased water-surface elevation (Fig. 6B). The sediment pulse in the middle reach dispersed downstream with the maximum change in water-surface elevation (+1.0 to +1.5 m) occurring early December 2012, January 2013, and April 2013 at Rkm 18.3, 15.3, and 13.5, respectively (Fig. 3B). After the peak of the bed material passed a given location, the stage lowered back to about +0.5 m above its pre-dam-removal elevation at Rkm 18.3 and 13.5 and back to its pre-removal elevation at Rkm 15.3 (Fig. 3B). High-frequency fluctuations (Fig. 3B, C) may or may not reflect actual changes in water-surface elevation. Such high-frequency fluctuations could result from differences in hydraulic control within the stage-gage network or localized perturbations to the water surface at the instrument location unrelated to aggradation. However, we interpret multi-week trends in measured water-surface elevation to represent real relative change in the hydraulic control reflecting bed aggradation or incision.

From 1–14 November 2012, the stage gage affected by the former Lake Aldwell reservoir delta (Rkm 12.4) indicated bed incision of about –0.4 m (Fig. 3B). This pattern of incision was consistent with field observations that former Lake Aldwell sediment knickpoints had become stranded during low late summer flow, then rapidly mobilized as river flow increased again in the fall, increasing transport capacity and instigating rapid upstream knickpoint migration (Fig. 3B). This incision at Rkm 12.4 was subsequently reversed at the same time as the stage increase from the leading edge of the sediment pulse was recorded at other gage locations upstream and downstream. Presumably this represented new bed material arriving from upstream in late November, sourced from the former Lake Mills. From December 2012 to July 2013 a slow, progressive incision continued to erode the bed at Rkm 12.4 (Fig. 3B) until the bed material peak had passed. Bed elevation at Rkm 12.4 stabilized through the remainder of the study interval at the same elevation as in early-mid-November 2012, indicating bed incision of about –0.4 m at the upstream end of the former Lake Aldwell reservoir delta (Fig. 3B).

In the lower reach, initial water surface elevation changes occurred within two weeks after the substantial Lake Mills sediment release (the first half of November 2012) at Rkm 5.5 and Rkm 0.6 (Fig. 3C). The stage gage at Rkm 3.8 showed negligible change during the study, indicating that this section of the river responded to the sediment influx largely as a transport reach. Stage at Rkm 5.5 increased between November 2012 and March 2013 to a relatively constant value of +0.6 to +0.7 m (relative to pre-dam-removal elevation) through September 2013 (Fig. 3C). Topographic surveys of reach 1 (which included the stage-gage location at Rkm 5.5) in September 2013 showed maximum bed aggradation of +1.5 m locally where new sediment

bars had formed (Figs. 4B, 5). The stage at Rkm 0.6 increased to a maximum of +1.3 m in May 2013. No water-surface elevations were available after May 2013 for Rkm 0.6 because bank erosion destroyed the pressure gage measuring water-surface elevation there. However, a topographic survey in reach 3, which included the stage-gage location at Rkm 0.6, showed that as of September 2013 the bed there had aggraded by +2.0 m across most of the channel width, filling a large pool (Figs. 4F, 6C). By summer 2013, all of the pools throughout the middle and lower Elwha River remained mostly filled with sediment (Fig. 6), and the lowest 1.5 km of the river had aggraded by more than +1 m even in the thalweg (Figs. 4F, 6C), decreasing the channel slope there; this backwater deposition occurred in response to a base-level increase where the lowermost river aggraded into the Strait of Juan de Fuca.

During the second year of dam removal, new sediment also accumulated in floodplain channels but at rates and with depositional styles different than in the main channel (Fig. 7). Floodplain channels whose upstream elevation was similar to that of the main channel accumulated sediment at approximately uniform thickness along their length as a result of downstream flow through the floodplain channel (Fig. 7A). Three of the eight floodplain channels accumulated sediment in this manner. The other five had inlet elevations that were higher than the mainstem channel and outlets that were lower than the mainstem channel (Fig. 7B), and thus received downstream flow only during moderate to high (overbank) river discharge. The downstream ends of those channels accumulated sediment from backwater effects of the mainstem flow, with relatively little deposition in their upstream sections (Fig. 7B). Of the eight floodplain channels surveyed, seven accumulated new sediment, to an average of +0.50 m (± 0.38 m) in the middle and lower reaches combined. Accumulated thickness varied according to distance from source and slope of the mainstem Elwha River (Fig. 7C). In the middle reach the average new sediment depth was greatest in the floodplain channels nearest to Glines Canyon Dam and generally decreased downstream. Average sediment depth in the lower-reach floodplain channels generally increased downstream, with the thickest deposits in floodplain channels nearest the mouth of the Elwha River (Fig. 7C).

4.2. Bed sediment grain size

The new sediment accumulating in the Elwha River system during dam removal was substantially finer grained than most of the pre-dam-removal riverbed. Pre-dam-removal samples (1994–2011) indicated a bed dominated by cobbles, with armoring evident immediately downstream from each dam (Fig. 8A). The earliest new deposition during dam removal involved thin deposits of sand and mud filling interstitial spaces between cobbles (winter 2011–2012), and thus the riverbed temporarily showed bimodal grain-size distribution in which a mean grain size measurement would not be informative (Draut and Ritchie, 2013; data not shown in Fig. 8). The lack of a basal fine sediment layer in many channel margin deposits as of spring 2013 (Draut and Ritchie, 2013) indicated that the initial 2011–2012 fine sediment deposits were eroded, at least locally, prior to arrival of the large sediment wave in 2012–2013. By late fall 2012 and thereafter, new sediment covered almost all previous exposures of the pre-dam-removal bed, such that the dominance of granule and pebble sizes as a mean grain size from November 2012 into 2013 (Fig. 8B) accurately represented the sediment that was present. Grain size in the control reach upstream from the former Lake Mills, in contrast, did not change (Fig. 8B).

Temporal trends in grain size (Fig. 8C, D) indicated general fining of bed sediment but with different patterns in the middle and lower reaches. The middle-reach bed grain size decreased almost immediately after abundant sand and coarser sediment was released past the Glines Canyon Dam site beginning in October 2012 (data from November 2012 in Fig. 8C). Grain size in the middle reach decreased from a range of –8 to –4 φ (small boulder to pebble) to –6 to 2 φ (cobble to medium sand; Fig. 8C). Riverbed grain size increased slightly in the middle

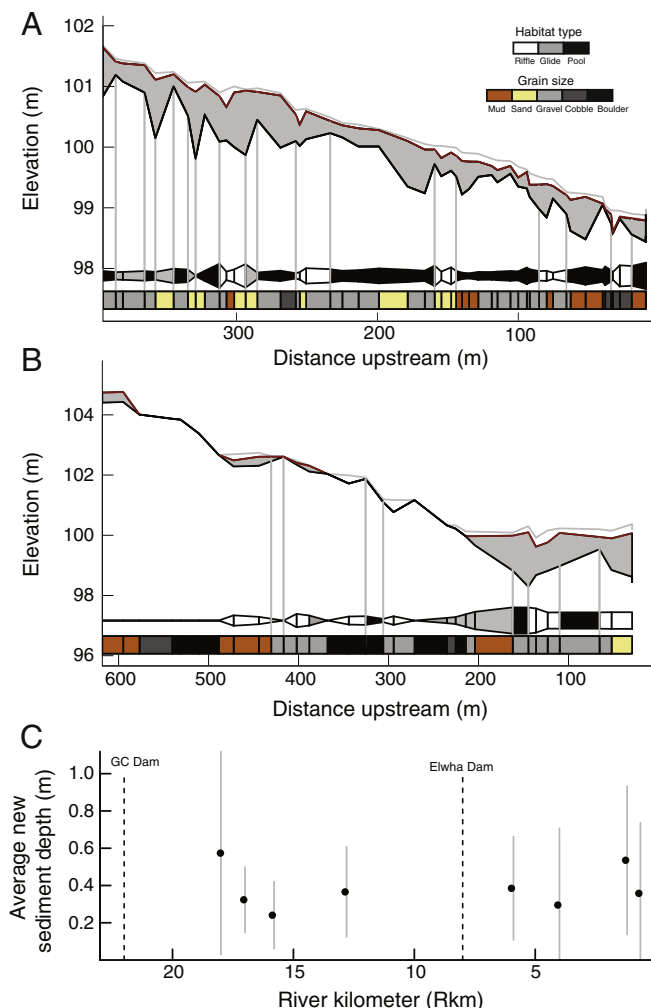


Fig. 7. Sediment accumulation in the floodplain channels of the middle and lower reaches as of summer 2013. (A) Floodplain channel accumulation example from Rkm 17.5, eastern portion of the floodplain, middle reach. Vertical lines (gray) denote beginning and end of each habitat unit, defined by water depth, velocity, and channel form. The top line (gray) is the water surface. The second line (brown) is the floodplain channel bed as defined by the top of newly accreted sediment. The third line (black) is the pre-dam-removal channel bed as defined by the base of the newly accreted sediment. The contracting and expanding bar is proportional to the wetted channel width at the time of the survey and colored according to habitat unit type prior to dam removal. The horizontal color bar on the bottom is colored by the dominant substrate in summer 2013. Note that sediment accumulation was widespread throughout the channel. (B) Floodplain channel accumulation example from Rkm 4.6, eastern portion of the floodplain, lower reach. Note that sediment accumulation was concentrated in the distal reach with little accumulation in the upstream portion of the floodplain channel. (C) Average sediment deposition (circles \pm standard deviation lines) in the eight studied floodplain channels of the Elwha River. Dashed lines denote dam locations.

reach in winter 2012–2013 and remained fairly constant through May–August 2013 (Fig. 8C). The lower reach showed a more consistent response in bed sediment grain size, fining less abruptly than in the middle reach (Fig. 8D); initial grain size there ranged from -10 to -4ϕ (boulder to pebble), but as of August 2013 had fined to between -6 and 2ϕ (cobble to medium sand), similar to the middle reach. Thus, grain size had decreased on the mainstem riverbed since the start of dam removal, but the rate of fining slowed or ceased after winter 2012–2013.

4.3. Channel planform adjustment

Mainstem sinuosity and braiding index of the middle and lower Elwha River showed changes coincident with the large sediment supply

increase during dam removal (Fig. 9). The most substantial channel planform changes followed the major bedload sediment release from the former Lake Mills in late 2012 (cf. Fig. 3). After that time, braiding index in the middle and lower reaches increased, reflecting new bar formation as sediment accumulated, and mainstem sinuosity also increased slightly (Fig. 9). Braiding index decreased between February and September 2013, more so in the middle river than in the lower river (Fig. 9B). This style and timing of channel planform response are consistent with the patterns of water-stage elevation described above (Fig. 3). Bank erosion occurred in some locations but was not widespread or pronounced enough to influence channel planform substantially.

4.4. Sediment accumulation estimates

We combined topographic, bed sediment, and channel-planform measurements to estimate the amount of new sediment in the Elwha River system after the first two years of dam removal (Table 1). Mainstem topographic change detected using terrestrial lidar and surveyed cross sections (method M1) within reach 1, the subreach in the lower river centered at Rkm 5.5, showed a volume increase of $9200 \pm 330 \text{ m}^3$ (uncertainty from thresholding to the 95% confidence interval) between September 2011 and September 2013, which equated to 54 m^3 of deposition per meter of river length (Fig. 5). Lidar scans and topographic surveys detected $1900 \pm 280 \text{ m}^3$ of volume increase in reach 2, within the old mainstem channel of the lower river (approximately equivalent to Rkm 2.6 on the mainstem), or $18 \text{ m}^3/\text{m}$ of channel length. In reach 3, centered at Rkm 0.6, we measured a volume increase of $14,000 \pm 680 \text{ m}^3$, or $130 \text{ m}^3/\text{m}$ of river length. In contrast to the strong depositional signal downstream from the former reservoirs, sediment volume was essentially unchanged in the control reach upstream from the former Lake Mills over the same time interval—the volume change there, 16 m^3 , was below our detection limit. Using method M1 and assuming a dry bulk density range of $1200\text{--}1700 \text{ kg/m}^3$, extrapolating mass accumulation along the lower reach and old mainstem channel (as described in Section 3.4) indicated $530,000\text{--}740,000 \text{ t}$ of new sediment in the lower river and old mainstem (Table 1A).

Using method M2 we measured a volume increase of $240,000 \pm 2500 \text{ m}^3$ in the middle Elwha River and $340,000 \pm 2100 \text{ m}^3$ in the lower river, or a total of about $580,000 \text{ m}^3$. Assuming a dry bulk density range of $1200\text{--}1700 \text{ kg/m}^3$, this indicated $690,000$ to $980,000 \text{ t}$ of new sediment stored within the active channel as of mid-September 2013 along 18 Rkm of the middle and lower river (including length along the mainstem, the old mainstem, and another major side channel; Table 1A). This represents an average new sediment thickness of 0.5 m in the middle reach and 0.8 m in the lower reach (thinner than shown in Fig. 4 because these values include deposition over former riffle crests), yielding average sediment storage of 27 and $39 \text{ m}^3/\text{m}$ of river length in the middle and lower river, respectively. The greater deposition in the lower reach is consistent with its lower gradient and modest increase in discharge. In the middle and the lower river, 60% of the new sediment was stored in bars that were subaerially exposed at low flows and 40% was below the water surface, mostly stored in former pools. Methods M1 and M2 yielded accumulation estimates for the lower river that overlapped (Table 1A), indicating that method M2 was a reasonably robust means to estimate sediment accumulation in the middle reach where high-resolution terrestrial lidar and total-station survey data were not available. We note that the uncertainty in our volume-to-mass conversion, resulting from the range of our bulk density assumptions, is two orders of magnitude greater than the uncertainty in our volume change calculations for methods M1 and M2.

In addition to the above estimates of sediment accumulation in the mainstem channel, we used topographic measurements from the eight studied floodplain channels (Fig. 7) to estimate total sediment accumulation in the 40 floodplain channels in the middle and lower reaches. Using the three methods described in Section 3.4 for floodplain

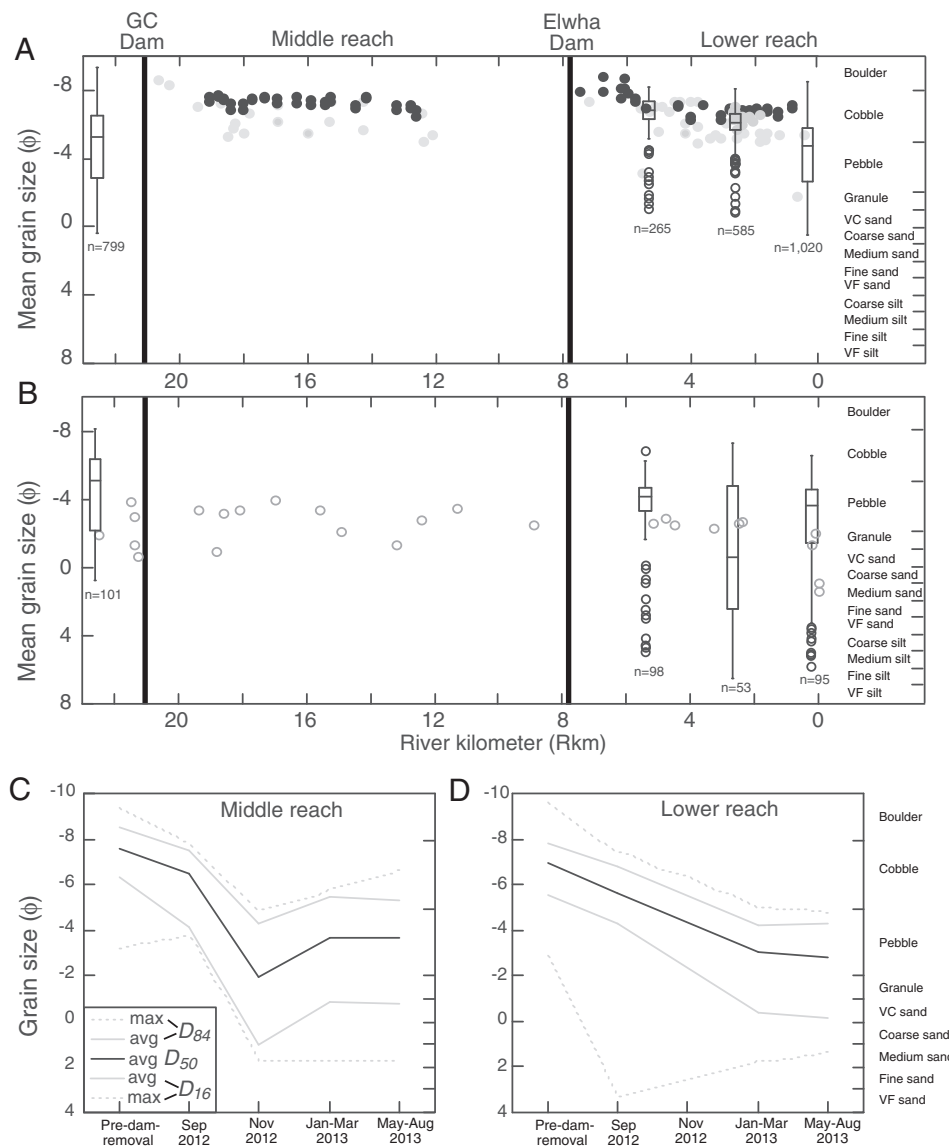


Fig. 8. Bed-sediment grain-size variation on the Elwha River in space and time. (A) and (B), spatial variation plotted for time aggregates of pre- and post-dam-removal; (C) and (D), temporal variation plotted for spatial aggregates of middle reach and lower reach (horizontal axis not to scale). (A) Black circles, pebble-counted samples from riffle crests. Gray circles, pebble-counted samples at locations other than riffle crests. Box-and-whisker plots, numerous samples within three subreaches in the lower reach, known as reaches 1, 2, and 3, and the control reach upstream from Lake Mills and Glines Canyon Dam (Draut et al., 2011), analyzed using the CobbleCam algorithm (Warrick et al., 2009). Box height spans interquartile range, horizontal line through box shows median, open circles represent data outlying by >1.5 times the interquartile range. (B) Open gray circles, bulk sediment samples from bars; box-and-whisker plots, samples within the subreaches of (A); in (B), all samples finer than medium sand were processed by laser particle size analysis. Time span covered by (A) includes 1994 to September 2011. Time span covered by (B) includes November 2012 to September 2013. Samples from September 2012 used in (C) and (D) are omitted from (A) and (B) to demonstrate the clear difference before and after bedload release began from the former Lake Mills in early November 2012. (C) Grain-size distribution shift through time for 37 samples from the middle reach. (D) Grain-size distribution shift through time for 41 samples from the lower reach. In (C) and (D), samples up to and including September 2012 are pebble counts; samples from November 2012 and thereafter are bulk sediment samples.

channel sediment accumulation, we estimate that between 94,000 and 310,000 t accumulated in the middle reach floodplain channels and between 62,000 and 200,000 t accumulated in the lower reach floodplain channels (Table 1B). The estimated range of total sediment accumulation in the middle and lower reach floodplain channels, which together are ~25 km long, is between 160,000 and 510,000 t (Table 1B).

Combining our estimates for mainstem and floodplain-channel accumulation (Table 1), we have documented at least 850,000 t of new sediment accumulation in the river system downstream from the dam sites, and possibly as much as 1.5 million t given the uncertainty range on these estimates (Table 1). Choosing the middle of the ranges of mass estimates in Table 1, we infer ~1.2 million t of new sediment accumulation in the mainstem and floodplain channels after the first two years of dam removal. This represents about 10% of the released reservoir sediment (Randle et al., 2014-in this volume), or about 14%

of the total suspended and bedload (a combined ~8.2 million t) in transport in the lower river during that time (Magirl et al., 2014-in this volume). Thus, most of the released reservoir sediment was transported downstream to the river mouth and coastal zone (see Gelfenbaum et al., 2014-in this volume).

5. Discussion

5.1. Geomorphic and sedimentary responses to dam removal

The geomorphic evolution of the Elwha River during the first two years of large-scale dam removal represented conditions rarely observed in natural river systems. The changes in topography, grain size, and channel planform resulted from a unique, artificially generated imbalance between sediment supply and transport capacity. Whereas

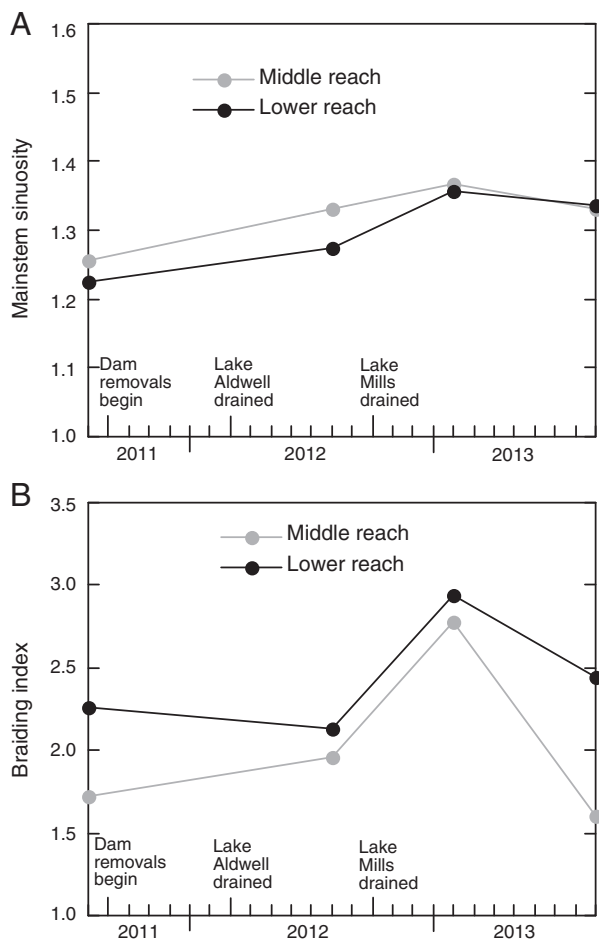


Fig. 9. Channel planform change on the Elwha River during dam removal. (A) Mainstem channel sinuosity in the middle and lower reaches, calculated as the midline length of the mainstem channel divided by straight-line, downvalley distance (7232 and 6156 m for middle reach and lower reaches, respectively). (B) Braiding index (Friend and Sinha, 1993), calculated as the sum of all channel lengths divided by mainstem channel length.

the river hydrology during dam removal was essentially natural and peak flows were lower than normal, the phased lowering of two reservoirs (Fig. 2) provided abundant reservoir sediment for fluvial transport (Curran et al., 2013; Magirl et al., 2014-in this volume; Randle et al., 2014-in this volume).

Downstream influence of a sediment wave (Fig. 3), widespread deposition in the mainstem and floodplain channels (Figs. 4–8), and

planform adjustments (Fig. 9)—which were all especially pronounced in the second year of dam removal following the major sediment release from the former Lake Mills—are attributable to excess sediment supply with respect to transport capacity. However, the geomorphic work available from the muted flood regime (no flows approaching the 2-year flood as of September 2013) restricted the spatial extent and potentially the magnitude of channel changes that might have occurred given a major flood event.

The Elwha River system showed relatively little response to the 1.1 million t of suspended sediment and estimated 160,000 t of bedload predominantly released from former Lake Aldwell by September 2012 (Magirl et al., 2014-in this volume). Over that first year of dam removal, new sediment did accumulate in the lower reach, particularly in the first 3 km downstream from the Elwha Dam site, but not in large enough quantities to alter channel morphology substantially (Fig. 9). Fine sediment was widely observed along the lower reach in spring and summer 2012, filling interstitial spaces in the cobble bed and building small (<0.2-m-thick) but ubiquitous lateral bars along the channel margins (Draut and Ritchie, 2013). New woody debris was also present along the lower Elwha River reach as of summer 2012, most of which had eroded from within the former reservoir deposits. During spring and summer 2012, sand and gravel filled pools in the lower reach (notably four large pools in the first 2.5 km downstream from the Elwha Dam site; Fig. 6C). Overall, relatively little sediment accumulated in the channel thalweg during the first year—observed sandy bedforms and gravel-pebble deposits in the thalweg were still generally <0.5 m thick as of July 2012—and there was no detectable accumulation then on riffle crests that provided hydraulic control to the stage-gage network (Fig. 3).

Much greater geomorphic response followed the sediment released during the second year of dam removal, predominately from the former Lake Mills, when extension of the sediment wave (Fig. 3) caused enough aggradation to cover even the riffle crests, fundamentally changing the riverbed from pool–riffle to braided morphology (Fig. 6). Widespread mainstem bed aggradation over the second year of dam removal (1–2 m throughout most of the mainstem channel) forced flow through floodplain channels even during low to moderate discharge, depositing additional sediment in the side channels of the Elwha River floodplain. New deposition in floodplain channels was particularly evident in the middle reach. Mainstem aggradation formed numerous bars, resulting in a more braided channel by February 2013 (Figs. 5, 9). Increased braiding on the Elwha River is consistent with observations in flume experiments of channel response to sediment pulses (Podolak and Wilcock, 2013) and on other rivers that accommodate a major sediment influx and have high suspended and bedloads (Smith and Smith, 1984; Schumm, 1985; Hoffman and Gabet, 2007; Gran, 2012; Mueller and Pitlick, 2013; Pierson and Major, 2014). New bar and channel formation

Table 1

Estimated sediment mass accumulation in the mainstem and floodplain channels of the middle and lower Elwha River during the first two years of dam removal (September 2011 to September 2013), in metric tonnes (t); estimates assume a dry bulk density range of 1200–1700 kg/m³ to convert sediment volume to mass; see text for complete method descriptions.

(A) Mainstem channel sediment accumulation using extrapolations from terrestrial lidar and high-resolution topographic surveys in three subreaches of the lower river (method M1) and using DEMs for the middle and lower river constructed from aerial lidar data, SfM data, and boat-mounted ADCP bathymetric surveys (method M2); the middle reach is ~9 km long and the lower reach is ~8 km long.

Location	Method M1	Method M2
Middle reach mainstem	N/A	280,000–410,000 t
Lower reach mainstem	530,000–740,000 t	410,000–580,000 t
Total mainstem	N/A	690,000–980,000 t

(B) Floodplain channel estimates using three different methods based on topographic surveys: simple volume estimate vs. aggregate volume measured (method F1), thalweg and cross section depth vs. thalweg estimate (method F2), and simple volume estimate vs. individual volume measured (method F3); in total, the 40 floodplain channels are ~25 km in length (all values are rounded and reported to two significant figures)

Location	Method F1	Method F2	Method F3
Floodplain channels of middle reach	94,000–130,000 t	150,000–210,000 t	220,000–310,000 t
Floodplain channels of lower reach	62,000–88,000 t	97,000–140,000 t	140,000–200,000 t
Total floodplain channels	160,000–220,000 t	240,000–340,000 t	270,000–510,000 t

also may have been facilitated by new deposition of large woody debris (cf. Fetherston et al., 1995; O'Connor et al., 2003; McHenry et al., 2007; Collins et al., 2012; Wohl, 2013). Bar formation and increased braiding through winter 2012–2013 represented a geomorphic shift from a river that had previously avulsed new channels by incising into preexisting floodplain deposits to one with new channels forming by aggradational-style avulsion (*sensu* Mohrig et al., 2000). New channel formation is seldom documented on field scales (Slingerland and Smith, 1998, 2003; Aslan et al., 2005; Sinha, 2009), but documenting the transition to a system forming new bars and reorganizing its channels purely as a result of greatly increased sediment supply, without flooding, is especially rare except in cases of extensive geomorphic disturbance (cf. Gilbert, 1917; Simon, 1999; Sutherland et al., 2002; Gran, 2012).

Flume studies and one-dimensional numerical analyses show that sediment-wave dynamics can be broken down into translational and dispersive components (Lisle et al., 2001). In an Eulerian reference frame, observing the river from a fixed point on the bank, both sediment-wave dispersion and translation would result in a rise and then fall of the riverbed or water-surface elevation. Sediment-wave translation and dispersion following dam removal have been documented where the sediment size is much finer than the downstream river bed and the Froude number ($Fr = u/(gd)^{0.5}$, where Fr is the nondimensional Froude number, u is mean water velocity, g is gravitational acceleration, and d is water depth) is small (Simons and Simons, 1991; Doyle et al., 2002; Stanley et al., 2002; Tullos et al., 2010). However, over the first two years of the Elwha River dam removal we did not detect widespread sediment-wave translation, but found that dispersion dominated. Lisle et al. (2001) argued that pure wave translation must demonstrate progressive downstream movement of the influence of the leading edge, apex, and trailing edge of the wave and that the trailing edge of the wave must return the river to a geomorphic condition similar to that present before the wave arrived. Data from our stage-gage network indicated that the apex of maximum deposition moved downstream from Rkm 18.3 to 13.5 in five months between December 2012 and April 2013. Translation of the leading and trailing edges of the sediment wave was more equivocal. The leading edge of influence of the sediment released from the former Lake Mills in October 2012 affected the entire stage-gage network within two weeks after 31 October 2012, and response was nearly synchronous throughout the middle reach. The trailing edge of the sediment wave appeared to affect Rkm 18.3 and 13.5 in a temporally similar pattern, whereas response at Rkm 15.3 seemed to indicate translational sediment-wave passage by June 2013 (Fig. 3B). In the lower reach, which favored deposition, we found neither evidence of apex translation nor strong indication of the trailing edge of the sediment wave as of September 2013 (Fig. 3C). Instead, comparison with theoretical and flume-based observations of Lisle et al. (2001) indicated that the sediment wave demonstrated dispersive properties. The patterns that we observed—pool filling, bed aggradation followed by degradation and incision, temporarily increased braiding, and bed sediment fining—are all consistent with sediment-wave dispersion (e.g., Lisle et al., 2001; Cui and Parker, 2005; Lisle, 2008; Pryor et al., 2011). The dominantly dispersive wave behavior (cf. Pizzuto, 2002) likely reflects the fact that the sediment wave was coarse-grained (largely sand and gravel) and that the river's hydraulic conditions tended toward higher Froude numbers. A cursory analysis of hydraulic data measured at the McDonald Bridge gage from November 2012 to May 2013 indicated Froude numbers ranging from 0.60 to 0.95, well above a suggested $Fr < 0.4$ threshold required to promote sediment wave translation (Lisle, 2008). Therefore, we consider the Elwha River sediment wave to be dominantly dispersive thus far; translational behavior may have been recorded at Rkm 15.3, but more data will be needed to assess that fully, as the geomorphic response of the river to completion of Glines Canyon Dam removal is further analyzed.

By September 2013 the primary effects of the first major sediment wave released from Lake Mills had decayed with passage of the wave

front, at least for the flow regime experienced thus far. Bed aggradation had given way to incision in the middle reach (Fig. 3B), and incision was observed in localized areas of the lower reach but was not yet well established there (Fig. 3C). Some, but not all, hydraulic controls (riffle and rapid crests) were re-exposed. Together with a decrease in braiding index relative to February 2013 (Fig. 9B), the tendency toward incision reflected the decay of the dispersing sediment wave. The sediment mass estimated for the river system (Table 1) therefore only represents one snapshot in time, that of late summer 2013; storage of new sediment in the river system will likely continue to decrease, with the exception of the lowest 0.5 Rkm where aggradation accompanied channel lengthening, base-level increase, and delta enlargement at the river mouth. It is uncertain to what extent a major flood would cause additional aggradation in the middle and lower reaches, having mobilized more reservoir sediment, or whether a large flood in the near future would have a net erosional effect on the river channel sediment storage. Removal of the remaining portion of Glines Canyon Dam over 2013–2014 also will affect downstream morphology.

The geomorphic response of the Elwha River to dam removal greatly exceeded the magnitude of geomorphic change caused by a major flood several years earlier, which was the largest forcing event measured there prior to dam removal. The 1016 m³/s flood of 3 December 2007, which had a recurrence interval of ~40 years, was the second-highest recorded discharge on the Elwha River (the highest having been 1177 m³/s in 1897). The 40-year flood caused major widening and channel reorganization upstream from Lake Mills, but induced relatively little change downstream from the dam sites, where the armored bed and low sediment supply limited channel movement (Draut et al., 2011). Bed elevations in the lowermost Elwha River (around Rkm 0.6, reach 3) locally increased and decreased by as much as 1.5 m in response to the 2007 flood but changed by 0.1–0.5 m elsewhere along the lower river (Draut et al., 2011). In contrast, the lower reach geomorphic signal from dam removal involved bed elevation changes that were two- to tenfold greater than those caused by the 40-year flood. The type of channel response possible during dam removal was also fundamentally different from that of any large forcing event (such as flooding or human channel realignment) during the dammed era because dam removal supplied so much new sediment, allowing bed fining and new bar formation that could not occur while the dams trapped sediment.

Before dam removal, a one-dimensional sediment transport modeling study (Konrad, 2009) projected patterns of bed aggradation and degradation on the Elwha River for time scales of 4–7 years after the start of dam removal. Insufficient time has elapsed to compare the field results directly with the time scales employed by the Konrad (2009) model runs; however, the state of the river two years after the start of dam removal largely conformed to model predictions, although Konrad (2009) anticipated great uncertainty because the model lacked topographic calibrations and a means to represent channel avulsions and assumed lower sediment volume than was present as of 2011. As Konrad (2009) projected, we found localized areas of net aggradation and degradation in the middle reach generally <1 m in magnitude (although 3–5 m of aggradation occurred in pools; Fig. 6B). In the lower reach, at 7 years after dam removal Konrad (2009) predicted the greatest bed aggradation around Rkm 5.5 (a +2 m increase relative to the pre-dam-removal elevation), attenuating downstream to negligible effects at the river mouth. Over decadal time scales, bed aggradation was anticipated to cover the lower reach more or less uniformly with ~1 m of new sediment, raising the 100-year flood stage by that amount (U.S. Department of Interior, 1996b; see also Gelfenbaum et al., 2011). Our data show that as of summer 2013 the riverbed elevation in the lower reach already exceeded the pre-dam-removal elevation by 0.6–1.0 m without showing any substantial downstream taper from Rkm 5.5. In addition, we found greater aggradation (~2 m) and lower channel slope from Rkm 1.5 to the river mouth (Figs. 4F, 6C), which was not included in numerical or conceptual predictions (Konrad, 2009; Gelfenbaum et al., 2011). The one-dimensional fluvial sediment

transport models were not able to simulate the substantial enlargement of the coastal delta (Gelfenbaum et al., 2014-in this volume), which raised base level enough to enhance sediment aggradation and decrease the slope in the lowermost Elwha River.

One difference between the predicted and measured responses concerned the behavior of muddy sediment (silt and clay). Mud deposition was anticipated to be negligible in the river system relative to the total volume of fines released (Randle et al., 1996), but channel-margin deposits as of spring 2013 contained, on average, around 20% mud (Draut and Ritchie, 2013). The unexpected abundance of silt and clay deposition is attributable to the great fine-grained sediment supply, coupled with unusually low fluvial transport capacity, having produced spatial and temporal flux gradients that promoted mud deposition. Although the 20% mud composition was locally a substantial proportion of total deposition, and some deposits contained a much greater mud proportion, the vast majority of fine sediment released from the reservoirs was transported to the river mouth as predicted. The new deposits likely will coarsen with time as the riverbed degrades through extension of the initial sediment wave (Madej et al., 2009; Pierson et al., 2011).

Although every dam removal involves unique geomorphic, sedimentary, and hydrologic conditions, it is nevertheless informative to consider lessons learned from the Elwha River dam removals in the context of the recent spate of dam removal research. Conditions affecting the Elwha River are unique compared to other dam removal projects, where sediment volumes were much less and peak flow hydrology relatively greater (e.g., Major et al., 2012; Woelfle-Erskine et al., 2012). During the first two years of dam removal on the Elwha River, sediment supply and concomitant bedload were exceptionally large and peak flow hydrology unusually small. This created a situation with greater sediment oversupply than had occurred at most other dam removals, though in the context of gradual, phased removal rather than the instantaneous large dam removals on several other rivers from which information is available. The most informative comparisons can be made between the Elwha River dam removals and those of Marmot Dam on the Sandy River, Oregon (Major et al., 2012), and Condit Dam on the White Salmon River, Washington (Wilcox et al., 2014), as those involved similar geographic and hydroclimatologic settings to the Elwha River and also involved no mechanical sediment removal. The magnitudes of the sediment pulses relative to the amount of stored reservoir sediment were similar in each case, although the erosion time scales and the magnitude of stored sediment relative to annual sediment load differed. The Elwha River eroded ~32% of its reservoir sediment over two years, representing decades' worth of the annual fluvial sediment load (Randle et al., 2014-in this volume); the Sandy River eroded ~58% of the reservoir sediment behind Marmot Dam over two years, representing 2–4 times the annual load (Major et al., 2012); the White Salmon River eroded ~55% of the reservoir sediment behind Condit Dam over 15 weeks, representing 50 times the annual sediment load (Wilcox et al., 2014).

In addition to the Elwha River dams having impounded much more sediment than in any previous dam removals, the Elwha River situation differed importantly from others such as the Marmot or Condit dam removal because the phased timing of removal of the Elwha dams resulted in a longer duration of sediment release and lower sediment concentrations. Measured peak suspended-sediment concentrations during instantaneous removal of Marmot Dam and Condit Dam were 3 times and 52 times greater, respectively, than those recorded on the Elwha River during the first two years of dam removal (49,000 mg/L at Marmot Dam and a hyperconcentrated flow of 850,000 mg/L at Condit Dam, compared to 16,300 mg/L from the Glines Canyon Dam removal on the Elwha River; Major et al., 2012; Wilcox et al., 2014; Magirl et al., 2014-in this volume), although sampling frequency was lower on the Elwha River than on those other rivers during instantaneous dam removal (Magirl et al., 2014-in this volume).

The phased removal of the Elwha dams meant that downstream sediment supply was controlled by fundamentally different processes than were important in the Marmot or Condit Dam removals. In the latter two cases, the sudden base level drop accompanying instantaneous dam removal led to rapid upstream propagation of major knickpoints or knickzones through the reservoir sediment, exerting a significant control on reservoir sediment erosion rate and thus sediment supply to the river below the dam sites. The reservoirs behind Marmot and Condit Dams had contained thick sediment deposits abutting the respective dams, facilitating rapid, large-magnitude knickpoint retreat upon dam removal (Major et al., 2012; Wilcox et al., 2014). Reservoir sediment erosion during the Condit Dam removal also largely proceeded by mass-movement processes in the dominantly fine-grained deposit (60% sand, 35% silt and clay, 5% gravel), which contributed to the hyperconcentrated flow mentioned above (Wilcox et al., 2014). The relative influence of knickpoint migration was less in the Elwha River reservoir deposits, owing to the more gradual base-level lowering that forced reservoir sediment deltas to prograde toward the dam sites over months before releasing bedload past them. Knickpoints did migrate upstream through the Elwha reservoir deposits after dam-notching events, but their elevation relative to the reservoir-deposit thickness was much less than that in instantaneous dam removals. Mass movement was rare or absent because the Elwha reservoir deposits were coarser and thus likely less cohesive than those behind Condit Dam (Randle et al., 2014-in this volume).

As a consequence of phased dam removal, the nature of reservoir erosion, and the reservoirs not having been full of sediment, the Elwha River sediment wave advanced downstream from the dam sites more slowly than in the Marmot or Condit examples, developing over weeks and influencing middle and lower reach locations for months before giving way to incision (Fig. 3). Those processes took only hours to days after the Condit Dam removal (Wilcox et al., 2014). Notably, the effects of the Elwha River sediment wave (i.e., fining of bed material) differed from those that can occur where instantaneous dam removal accompanies a large flood flow; the failure of Barlin Dam, Taiwan, during a typhoon-induced flood in 2007 resulted in coarsening, rather than fining, of bed sediment downstream from the dam site (Tullos and Wang, 2014). The balance between sediment supply and transport capacity will determine the extent of deposition or erosion and relative grain-size changes, with resulting deposits and channel configurations that are highly variable from one example to another.

Despite the important differences of phased vs. instantaneous large dam removal, and the associated differences in sediment-supply mechanisms and sediment-wave timing, certain similarities are apparent among the Elwha, Condit, and Marmot case studies. In each case the fluvial system digested a substantial sediment pulse fairly efficiently, moving the great majority of the sediment downstream out of the respective study reaches (5–10 km long) rather than retaining much of it near the dam sites (cf. Major et al., 2012; Warrick et al., 2014-in this volume). Even in view of the uncertainties on sediment budgeting, our finding of about 10% retention of eroded reservoir sediment in the Elwha River system is comparable to results from a similar-length reach downstream from Marmot Dam (Major et al., 2012; a detailed sediment budget is not available for the Condit Dam removal). Thus, these river systems appear remarkably resilient from a sedimentary and geomorphic perspective. Moreover, large quantities of sediment evidently can move downstream after dam removals even without the influence of substantial flood hydrology, as long as stream power is sufficient to mobilize reservoir sediment. Much greater geomorphic change occurred downstream from the Marmot Dam site in the first year after dam removal, under a relatively low flow regime (peak flow having been 60% of a 2-year flow) but during dynamic knickpoint migration through the reservoir deposit than in the second year under the influence of a 10-year flood. This similarity with the sediment-wave dispersion on the Elwha River under modest hydrologic conditions suggests that flow sequencing may be less important than dam-

removal rate and reservoir sediment erosion mechanisms in controlling geomorphic change after dam removal (Grant et al., 2012). Additional data collection over longer time scales on the Elwha River and other dam-removal settings should substantially increase understanding of the relative roles of various geomorphic and hydrologic forcing mechanisms.

Even though the majority of eroded reservoir sediment from the former Lakes Aldwell and Mills moved downstream to the coast, some effects of the dam-removal sediment wave on the Elwha River likely will be long-lasting. Judging from comparison with natural sediment pulses, the full sedimentary and geomorphic responses of the Elwha River to dam removal could last for decades, and possibly more than a century (cf. Pierson et al., 2011; Pierson and Major, 2014). Although river and floodplain form and function were impaired by the upstream dams, e.g., with bed armoring in the channel and unnatural vegetation age distribution on the floodplain (Pohl, 2004; Kloehn et al., 2008; Draut et al., 2011), the river channel and floodplain apparently had not finished equilibrating to the sediment-limiting effects of the dams after almost a century, at least in the lowest 4 km of the river (Draut et al., 2011). Therefore, a similarly long, nonlinear post-dam-removal response may occur as the river accommodates not only the wave of reservoir sediment measured in this study, but also the reestablishment of natural sediment supply from the upper watershed. As that happens, we expect that the river will host a greater range of bed sediment grain size compared to the pre-dam-removal bed and that the active, unvegetated channel width will increase over time (cf. Kondolf et al., 2002). We have not discussed channel width changes in detail here; preliminary data from reach 1 indicate that wetted width in September 2013 was ~5–10% greater than at comparable discharge before dam removal, and we have observed bank erosion and widening locally in the middle and lower river, but until the Elwha River experiences at least a 2-year flood after dam removal it is not meaningful to compare active channel width to that measured before dam removal. We speculate that sediment loads from the former reservoirs will approach a stable recruitment level for a given flow regime within a few years after the end of dam removal and the occurrence of two to three floods equal to or greater than the 2-year flood. This prediction depends partly on additional mobilization of reservoir sediment during larger peak flow events (cf. the post-dam-removal ‘event-driven phase’ of Pearson et al., 2011, and the Marmot Dam example discussed above; Major et al., 2012) and is supported numerically by Konrad (2009). Continued reservoir sediment erosion is also expected to influence channel deposits and morphology downstream of the dam sites as fine-grained lakebed deposits become exposed that had not yet eroded substantially as of 2013 (Warrick et al., 2014-in this volume). Sediment in excess of the pre-dam-removal state will continue to be present in downstream regions (the middle and lower river) as a result of successful restoration of sediment delivery from the upper watershed and of continued recruitment from the former reservoir areas (albeit at a more stable, reduced level).

5.2. Ecological implications

A dearth of long-term data sets (Doyle et al., 2005; Jackson and Füreder, 2006) makes it difficult to predict how long the ecological effects of dam removal will last (e.g., Harding et al., 1998; Bednarek, 2001; Vinson, 2001). The Elwha River dam removals were designed to restore habitat for anadromous fish species whose populations declined significantly over the century that the dams were in place (Beechie et al., 2001; Brenkman et al., 2008, 2012; Pess et al., 2008; Kocovsky et al., 2009). Many complex, long-lasting ecological effects of this river restoration are anticipated (e.g., Duda et al., 2008), and a detailed consideration of these is outside the scope of this paper. However, we briefly consider some potential ecological implications of the new sediment deposition and its effects on habitat in mainstem and floodplain channels and bars.

During the first year of dam removal, before the major sediment influx from the former Lake Mills, suspended sediment from both reservoirs formed thin (<0.2 m), sand-and-mud deposits along most of the mainstem channel margin in the middle and lower Elwha River, filling interstitial spaces in the armored cobble bed surface (Draut and Ritchie, 2013). Maintenance of natural and functioning interstitial spaces is ecologically important, as these areas sustain habitat heterogeneity for macroinvertebrates (e.g., Wood and Armitage, 1997; Jones et al., 2012), facilitate hyporheic exchange (Harvey and Bencala, 1993), and trap organic material. The filling of riffles and pools can decrease the density of macroinvertebrates (Minshall et al., 2001; Gayraud and Philippe, 2003; Thompson et al., 2005; Clayton and Westbrook, 2008) and affect their community structure (e.g., Kaller and Hartman, 2004; but see Stanley et al., 2002). Morley et al. (2008) postulated that periphyton and benthic invertebrate abundance and diversity would decrease temporarily as a response to the Elwha River dam removal, as a result of fine sediment burying cobbles, limiting photosynthesis via increased turbidity and decreasing the efficiency of filter-feeding organisms (cf. Wood and Armitage, 1997). Although we do not yet know the actual effects on those biotic communities, the sediment effects that we documented are consistent with those predicted to impact them.

Reduced pore space owing to fine sediment influx into bed interstices also limits the flow of oxygenated water through riverbed material, decreasing at least temporarily the amount of suitable fish-spawning habitat and reducing the viability of incubating fish eggs (Lisle, 1989; Bjorn and Reiser, 1991; Greig et al., 2005). Similar fine sediment infiltration downstream from the Milltown Dam site, Montana, persisted for several years after that dam removal (Evans and Wilcox, 2014). Pess et al. (2008) and McHenry and Pess (2008) anticipated an immediate short-term reduction in spawning-habitat quality downstream from the dams owing to an influx of fine sediment. Early fine sediment (fine sand and mud) infiltration of the Elwha River cobble bed was overwhelmed by the greater magnitude, coarser (coarser sand, granule, and pebble) sediment wave that caused much more aggradation in the second year (2012–2013). However, the earlier timing of fine sediment infiltration, together with elevated suspended-sediment loads compared to the pre-dam-removal condition, meant that substantial ecosystem impacts in the Elwha River preceded the arrival of the major sediment wave by about a year. By summer 2013, grain size on the main channel bed was dominantly granule and pebble material (Fig. 8), which, although still evolving, represented an increased proportion of anadromous fish spawning habitat compared to the too coarse cobble bed before dam removal or the too fine mud and sand bed of 2011–2012 (Kondolf and Wolman, 1993; see also Riebe et al., 2014).

Floodplain channels were conjectured to become either areas of fish habitat refuge if channels were protected from the major sediment wave in the mainstem river or areas of sediment accumulation if there was direct hydrologic connectivity between the mainstem and floodplain channels (McHenry and Pess, 2008; Pess et al., 2008). As of the second year of dam removal, seven of the eight floodplain channels measured in the middle and lower reaches were areas of new sediment deposition. The floodplain channel bed aggradation reduced the residual habitat depth and thus reduced juvenile salmon habitat capacity. However, the newly developed braids and smaller channels within the mainstem may provide some additional habitat complexity, as the grain size of sediment in those channels varies according to conditions at the bifurcations.

Finally, the increased area and finer grain sizes of bars in the first two years of dam removal have implications for riparian vegetation dynamics along the Elwha River. Pioneer trees and shrubs colonize bars, which commonly initiates a biophysical progression of landforms and associated riparian vegetation (Latterell et al., 2006; Naiman et al., 2010). Young stands comprised an unnaturally small proportion of riparian forest along the Elwha River downstream from the dams before removal, relative to reference streams (Kloehn et al., 2008). The increased bar area,

along with ongoing and potential future changes to channel planform, could trigger regeneration of woody riparian species, altering the age structure of the forest. We have already observed an increase in seedlings of common pioneer trees and shrubs on new bars along the middle and lower Elwha River. The relatively finer substrate of the post-dam-removal sediment deposits likely will favor some species over others and thus could influence riparian plant species composition (Shafroth et al., 2002b). Anticipated future increases in floodplain sediment deposition could influence existing riparian forests through differences in species tolerance to burial and by resetting understory plant communities.

6. Conclusions

Removal of two large dams on the Elwha River, Washington, provided a rare opportunity to quantify field-scale fluvial response to a major sediment influx. The dam-removal sediment pulse initially caused widespread bed aggradation of ~1 m (locally greater where pools filled), changing the river from pool-riffle to braided morphology and decreasing the slope of the lowermost 1.5 km of the river in response to increased base level from delta enlargement at the river mouth. Two years after the start of dam removal, 10.5 million t (7.1 million m³) of sediment, representing several decades worth of accumulation, had been released from the two former reservoirs. Of the sediment released, ~1.2 million t (about 10%) was stored along 18 river km of the mainstem channel and 25 km of floodplain channels. The Elwha River thus transported most of the released sediment to the river mouth.

The large sediment wave from the former Lake Mills reservoir dispersed downstream consistent with observations and predictions of sediment-wave dynamics in high Froude number rivers with coarse-grained sediment waves. Sediment-wave translation also may have occurred, but analysis of more data from later years of the dam-removal project will be required to assess how influential sediment-wave translation might be in influencing downstream fluvial geomorphology.

Newly deposited sediment in the mainstem river and floodplain channels, dominantly pebbles, granules, and sand, formed new bars and increased channel braiding, causing a transition to aggradational channel avulsion. As a result of mainstem bed aggradation, many side channels in the Elwha River floodplain accumulated new sediment and received surface water flow even during nonflood conditions. The river system showed a two- to tenfold greater geomorphic response to dam removal, in terms of bed elevation changes, than to a 40-year flood event four years before dam removal. Within one year of major sediment influx, the river began incising the newly deposited sediment as the initial sediment wave decayed, and some hydraulic controls (riffle and rapid crests) were re-exposed. Geomorphic alterations and changing bed-sediment grain size have important ecological implications, affecting aquatic habitat structure, benthic fauna, salmonid fish spawning and rearing potential, and riparian vegetation.

The Elwha River dam removals represent a unique case among the few examples of large dam removals described in the scientific literature. In addition to involving larger structures and substantially greater sediment volumes, the staged removal of the Elwha River dams resulted in a longer-duration sediment release and lower sediment concentrations than in other recent examples of instantaneous large dam removal. Sediment release to the Elwha River channel and floodplain also was controlled by different geomorphic processes than observed in other large dam removals—gradual progradation of reservoir deltas and eventual bedload transport past the dam sites months after removal began, rather than rapid, large-scale knickpoint propagation or mass movements that mobilized reservoir sediment during instantaneous dam removals. Whether large dam removal is phased or instantaneous, the case studies to date indicate that rivers are remarkably resilient to large-scale sediment pulses, efficiently transporting most new sediment downstream (given sufficient stream power). Even so, the relatively

small proportion of reservoir sediment that remains in the Elwha River channel and floodplain, together with renewed natural sediment and wood supply from the upper watershed, may affect the fluvial system for decades, with the riverscape topography, bed material, channel planform, and associated habitat structure substantially different than during the dammed era.

Acknowledgments

This study was funded by the National Park Service, U.S. Bureau of Reclamation, U.S. Geological Survey, and National Oceanic and Atmospheric Administration. We also acknowledge valuable discussions among colleagues through the USGS John Wesley Powell Center for Analysis and Synthesis working group on dam removal (2013–2015). The use of trade and company names in this publication is for descriptive purposes only and does not constitute endorsement by the U.S. Government. We thank A. Geffre, H. Hugunin, S. Kimbrel, P. Perkins, K. Wille, and numerous volunteers for their contributions to fieldwork on the Elwha River and related data analysis. A. Tan processed sediment samples in the USGS sediment laboratory, Santa Cruz, CA. J.J. Major, L. Harrison, J.A. Warrick, G.R. Gelfenbaum, B. Free, J.E. O'Connor, J.W. Lauer, and V. Leung are thanked for their discussions and comments on this manuscript. T.E. Lisle, M.A. Collins, one anonymous reviewer, and editor R.A. Marston provided thorough, constructive comments that improved the paper.

References

- Acker, S.A., Beechie, T.J., Shafroth, P.B., 2008. Effects of a natural dam-break flood on geomorphology and vegetation on the Elwha River, Washington, U.S.A. *Northwest Sci.* 82 (Special Issue), 210–223.
- American Rivers, 2014. Dam Removals Accessed 7 July 2014 <http://www.americanrivers.org/initiative/dams/projects/2013-dam-removals/>.
- Antevs, E., 1952. Arroyo-cutting and filling. *J. Geol.* 60, 375–385.
- Ashworth, P.J., Best, P.L., Jones, M., 2004. Relationship between sediment supply and avulsion frequency in braided rivers. *Geology* 32, 21–24.
- Aslan, A., Autin, W.J., Blum, M.D., 2005. Causes of river avulsion: insights from the late Holocene avulsion history of the Mississippi River, USA. *J. Sediment. Res.* 75, 650–664.
- Bednarek, A.T., 2001. Undamming rivers: a review of the ecological impacts of dam removal. *Environ. Manag.* 27, 803–814.
- Beechie, T.J., Collins, B.D., Pess, G.R., 2001. Holocene and recent geomorphic processes, land use, and salmonid habitat in two North Puget Sound river basins. *Water Sci. Appl.* 4, 37–54.
- Beechie, T.J., Liermann, M., Pollock, M.M., Baker, S., Davies, J., 2006. Channel pattern and river-floodplain dynamics in forested mountain river systems. *Geomorphology* 78, 124–141.
- Benda, L., Dunne, T., 1997. Stochastic forcing of sediment routing and storage in channel networks. *Water Resour. Res.* 33, 2865–2880.
- Bjorn, T.C., Reiser, D.W., 1991. Habitat requirements of salmonids in streams. In: Meehan, W.R. (Ed.), *Influences of Forest and Rangeland Management on Salmonid Fishes and Their Habitats*. American Fisheries Society, Bethesda, Maryland (Special Publication 19).
- Bouyoucos, J.A., Lai, Y.G., Randle, T.J., 2013. Sediment impacts from the Savage Rapids Dam removal, Rogue River, Oregon. In: De Graaff, J.V., Evans, J.E. (Eds.), *Geological Society of America Reviews in Engineering Geology* 21, pp. 93–104. [http://dx.doi.org/10.1130/2013.4121 \(08\).](http://dx.doi.org/10.1130/2013.4121 (08).)
- Brasington, J., Langham, J., Rumsby, B., 2003. Methodological sensitivity of morphometric estimates of coarse fluvial sediment transport. *Geomorphology* 53, 299–316.
- Braudrick, C.A., Dietrich, W.E., Leverich, G.T., Sklar, L.S., 2009. Experimental evidence for the conditions necessary to sustain meandering in coarse-bedded rivers. *Proc. Natl. Acad. Sci.* 106, 16936–16941.
- Brenkman, S.J., Pess, G.R., Torgersen, C.E., Kloehn, K.K., Duda, J.J., Corbett, S.C., 2008. Predicting recolonization patterns and interactions between potamodromous and anadromous salmonids in response to dam removal in the Elwha River, Washington state, USA. *Northwest Sci.* 82 (Special Issue), 91–106.
- Brenkman, S.J., Duda, J.J., Torgersen, C.E., Welty, E., Pess, G.R., Peters, R., McHenry, M.L., 2012. A riverscape perspective of Pacific salmonids and aquatic habitats prior to large-scale dam removal in the Elwha River, Washington, USA. *Fish. Manag. Ecol.* 19, 36–53.
- Burroughs, B.A., Hayes, D.B., Klomp, K.D., Hansen, J.F., Mistak, J., 2009. Effects of Stronach dam removal on fluvial geomorphology in the Pine River, Michigan, United States. *Geomorphology* 110, 96–107.
- Casalbore, D., Chiocci, F.L., Mugnozza, G.S., Tommasi, P., Sposato, A., 2011. Flash-flood hyperpycnal flows generating shallow-water landslides at Fiumara mouths in western Messina Strait (Italy). *Mar. Geophys. Res.* 32, 257–271.
- Cheng, F., Granata, T., 2007. Sediment transport and channel adjustments associated with dam removal: field observations. *Water Resour. Res.* 43, W03444. <http://dx.doi.org/10.1029/2005WR004271>.

- Chien, N., 1985. Changes in river regime after the construction of upstream reservoirs. *Earth Surf. Process. Landf.* 10, 143–159.
- Childers, D., Kresch, D.L., Gustafson, S.A., Randle, T.J., Melena, T., Cluer, B., 2000. Hydrological data collected during the 1994 Lake Mills drawdown experiment, Elwha River, Washington. U.S. Geological Survey Water Resources Investigations Report 99-4215, p. 115.
- Clayton, J.A., Westbrook, C.J., 2008. The effect of the Grand Ditch on the abundance of benthic invertebrates in the Colorado River, Rocky Mountain National Park. *River Res. Appl.* 24, 975–987.
- Collier, M., Webb, R.H., Schmidt, J.C., 1996. Dams and rivers: a primer on the downstream effects of dams. U.S. Geological Survey Circular 1126, p. 94 (Reston, VA).
- Collins, B.D., Montgomery, D.R., Fetherston, K.L., Abbe, T.B., 2012. The floodplain large-wood cycle hypothesis: a mechanism for the physical and biotic structuring of temperate forested alluvial valleys in the North Pacific coastal ecoregion. *Geomorphology* 139–140, 460–470.
- Covault, J.A., Craddock, W.H., Romans, B.W., Fildani, A., Gosai, M., 2013. Spatial and temporal variations in landscape evolution: historic and longer-term sediment flux through global catchments. *J. Geol.* 121, 35–56.
- Cowie, P.A., Whittaker, A.C., Attal, M., Roberts, G., Tucker, G.E., Ganas, A., 2008. New constraints on sediment-flux-dependent river incision: implications for extracting tectonic signals from river profiles. *Geol. Soc. Am. Bull.* 36, 535–538.
- Cui, Y., Parker, G., 2005. Numerical model of sediment pulses and sediment-supply disturbances in mountain rivers. *J. Hydraul. Eng.* 131. [http://dx.doi.org/10.1061/\(ASCE\)0733-9429\(2005\)131:8\(646\)](http://dx.doi.org/10.1061/(ASCE)0733-9429(2005)131:8(646)).
- Cui, Y., Parker, G., Lisle, T.E., Gott, J., Hansler-Ball, M.E., Pizzuto, J.E., Allmendinger, N.E., Reed, J.E., 2003a. Sediment pulses in mountain rivers: 1. Experiments. *Water Resour. Res.* 39, 1239. <http://dx.doi.org/10.1029/2002WR001803>.
- Cui, Y., Parker, G., Pizzuto, J., Lisle, T.E., 2003b. Sediment pulses in mountain rivers: 2. Comparison between experiments and numerical predictions. *Water Resour. Res.* 39 (9), 1240. <http://dx.doi.org/10.1029/2002WR001805>.
- Curran, C.A., Konrad, C.P., Higgins, J.L., Bryant, M.K., 2009. Estimates of sediment load prior to dam removal in the Elwha River, Clallam County, Washington. U.S. Geological Survey Scientific Investigations Report 2009-5221, 18.
- Curran, C.A., Magirl, C.S., Duda, J.J., 2013. Suspended-sediment concentration during dam decommissioning in the Elwha River, Washington. U.S. Geological Survey Data Set <http://dx.doi.org/10.5066/F7M043DB> (<http://wa.water.usgs.gov/pubs/misc/elwha/ssc/>).
- Czuba, C.R., Randle, T.J., Bountry, J.A., Magirl, C.S., Czuba, J.A., Curran, C.A., Konrad, C.P., 2011. Anticipated sediment delivery to the lower Elwha River during and following dam removal. In: Duda, J.J., Warrick, J.A., Magirl, C.S. (Eds.), *Coastal Habitats of the Elwha River, Washington—Biological and Physical Patterns and Processes Prior to Dam Removal*. U.S. Geological Survey Scientific Investigations Report 2011-5120, pp. 27–46.
- Czuba, J.A., Magirl, C.S., Czuba, C.R., Curran, C.A., Johnson, K.H., Olsen, T.D., Kimball, H.K., Gish, C.C., 2012. Geomorphic analysis of the river response to sedimentation downstream of Mount Rainier, Washington. U.S. Geological Survey Open-file Report 2012-1242 (134 pp.).
- Dade, W.B., Renshaw, C.E., Magilligan, F.J., 2011. Sediment transport constraints on river response to regulation. *Geomorphology* 126, 245–251.
- Dietrich, W.E., Kirchner, J.W., Ikeda, H., Iseya, F., 1989. Sediment supply and the development of the coarse surface layer in gravel-bedded rivers. *Nature* 340, 215–217.
- Doyle, M.W., Stanley, E.H., Harbor, J.M., 2002. Geomorphic analogies for assessing probable channel response to dam removal. *J. Am. Water Res. Assoc.* 38 (6), 1567–1579.
- Doyle, M.W., Stanley, E.H., Orr, C.H., Selle, A.R., Sethi, S.A., Harbor, J.M., 2005. Stream ecosystem response to small dam removal: lessons from the heartland. *Geomorphology* 71, 227–244.
- Draut, A.E., 2012. Effects of river regulation on aeolian landscapes, Colorado River, southwestern USA. *J. Geophys. Res. Earth Surf.* 117 (F2). <http://dx.doi.org/10.1029/2011JF002329>.
- Draut, A.E., Ritchie, A.C., 2013. Sedimentology of new fluvial deposits on the Elwha River, Washington, USA, formed during large-scale dam removal. *River Res. Appl.* <http://dx.doi.org/10.1002/rra.2724>.
- Draut, A.E., Logan, J.B., Mastin, M.C., 2011. Channel evolution on the dammed Elwha River, Washington, USA. *Geomorphology* 127, 71–87.
- Duda, J.J., Freilich, J.E., Schreiner, E.G., 2008. Baseline studies in the Elwha River ecosystem prior to dam removal. *Northwest Sci. 82* (Special Issue), 1–12.
- Duda, J.J., Coe, H.J., Morley, S.A., Kloehn, K.K., 2011. Establishing spatial trends in water chemistry and stable isotopes ($\delta^{15}\text{N}$ and $\delta^{13}\text{C}$) in the Elwha River prior to dam removal and salmon recolonization. *River Res. Appl.* 27, 1169–1181. <http://dx.doi.org/10.1002/rra.1413>.
- Dynesius, M., Nilsson, C., 1994. Fragmentation and flow regulation of river systems in the northern third of the world. *Science* 266, 753–762.
- Egozi, R., Ashmore, P., 2008. Defining and measuring braiding intensity. *Earth Surf. Process. Landf.* 33, 2121–2138.
- Eschner, T.R., Hadley, R.F., Crowley, K.D., 1983. Hydrologic and morphologic changes in the Platte River basin: a historical perspective. U.S. Geol. Surv. Prof. Pap. 1277-A, 39.
- Evans, E., Wilcox, A.C., 2014. Fine sediment infiltration dynamics in a gravel-bed river following a sediment pulse. *River Res. Appl.* 30, 372–384. <http://dx.doi.org/10.1002/rra.2647>.
- Fetherston, K.L., Naiman, R.J., Bilby, R.E., 1995. Large woody debris, physical processes, and riparian forest development in montane river networks of the Pacific Northwest. *Geomorphology* 13, 133–144.
- Friend, P.F., Sinha, R., 1993. Braiding and meandering parameters. In: Best, J.L., Bristow, C.S. (Eds.), *Braided Rivers*. Geological Society of London, London, U.K., pp. 105–111 (Special Publication 75).
- Galay, V.J., 1983. Causes of river bed degradation. *Water Resour. Res.* 19, 1057–1090.
- Gayraud, S., Philippe, M., 2003. Influence of bed-sediment features on the interstitial habitat available for macroinvertebrates in 15 French streams. *Int. Rev. Hydrobiol.* 88, 77–93.
- Geiger, A.F., 1963. Developing sediment storage requirements for upstream retarding reservoirs. Proceedings of the Federal Interagency Sediment Conference, U.S. Department of Agriculture, Washington, D.C. (pp. 881–885, USDA-ARS Miscellaneous Publication 970).
- Gelfenbaum, G., Duda, J.J., Warrick, J.A., 2011. Summary and anticipated responses to Elwha River dam removal. In: Duda, J.J., Warrick, J.A., Magirl, C.S. (Eds.), *Coastal Habitats of the Elwha River, Washington—Biological and Physical Patterns and Processes Prior to Dam Removal*. U.S. Geological Survey Scientific Investigations Report 2011-5120, pp. 249–263.
- Gelfenbaum, G.R., Stevens, A., Miller, I., Warrick, J.A., 2014. Large-scale dam removal on the Elwha River, Washington, USA: coastal geomorphic change. *Geomorphology* (in this volume).
- Gilbert, G.K., 1917. Hydraulic-mining debris in the Sierra Nevada. U.S. Geol. Surv. Prof. Pap. 105, 188.
- Grams, P.E., Schmidt, J.C., Topping, D.J., 2007. The rate and pattern of bed incision and bank adjustment on the Colorado River in Glen Canyon downstream of Glen Canyon dam, 1956–2000. *Geol. Soc. Am. Bull.* 119, 556–575.
- Gran, K.B., 2012. Strong seasonality in sand loading and resulting feedbacks on sediment transport, bed texture, and channel planform at Mount Pinatubo, Philippines. *Earth Surf. Process. Landf.* 37 (9), 1012–1022. <http://dx.doi.org/10.1002/esp.3241>.
- Grant, G.E., Schmidt, J.C., Lewis, S.L., 2003. A geological framework for interpreting downstream effects of dams on rivers. *Water Sci. Appl.* 7, 209–225.
- Grant, G.E., O'Connor, J.E., Major, J.J., 2012. The remains of the dam: what have we learned from 10 years of dam removal? American Geophysical Union, Fall Meeting, Abstract EP54C-08.
- Greig, S.M., Sear, D.A., Carling, P.A., 2005. The impact of fine sediment accumulation on the survival of incubating salmon progeny: implications for sediment management. *Sci. Total Environ.* 344, 241–258.
- Guthrie, R., Friele, P., Allstadt, K., Roberts, N., Evans, S., Delaney, K., Roche, D., Clague, J., Jakob, M., 2012. The 6 August 2010 Mount Meager rock slide-debris flow, Coast Mountains, British Columbia: characteristics, dynamics, and implications for hazard and risk assessment. *Nat. Hazards Earth Syst. Sci.* 12, 1277–1294.
- Harding, J.S., Benfield, E.F., Bolstad, P.V., Helfman, G.S., Jones III, E.B.D., 1998. Stream biodiversity: the ghost of land use past. *Proc. Natl. Acad. Sci.* 95, 14843–14847.
- Harvey, J.W., Bencala, K.E., 1993. The effect of streambed topography on surface-subsurface water exchange in mountain catchments. *Water Resour. Res.* 29, 89–98.
- Harwood, K., Brown, A.G., 1993. Fluvial processes in a forested anastomosing river: flood partitioning and changing flow patterns. *Earth Surf. Process. Landf.* 18, 741–748.
- Hazel Jr., J.E., Topping, D.J., Schmidt, J.C., Kaplinski, M., 2006. Influence of a dam on fine-sediment storage in a canyon river. *J. Geophys. Res.* 111 (F3). <http://dx.doi.org/10.1029/2004JF000193>.
- Hoffman, D.F., Gabet, E.J., 2007. Effects of sediment pulses on channel morphology in a gravel-bed river. *Geol. Soc. Am. Bull.* 119, 116–125.
- Howard, A.D., Keetch, M.E., Vincent, C.L., 1970. Topological and geomorphic properties of braided streams. *Water Resour. Res.* 6, 1647–1688.
- Jackson, J.K., Füreder, L., 2006. Long-term studies of freshwater macroinvertebrates: a review of the frequency, duration, and ecological significance. *Freshw. Biol.* 51, 591–603.
- James, L.A., 1989. Sustained storage and transport of hydraulic gold mining sediment in the Bear River, California. *Ann. Assoc. Am. Geogr.* 79, 570–592.
- Javernick, L., Brasington, J., Caruso, B., 2014. Modeling the topography of shallow braided rivers using Structure-from-Motion photogrammetry. *Geomorphology* 213, 166–182.
- Jerolmack, D.J., Paola, C., 2007. Complexity in a cellular model of river avulsion. *Geomorphology* 91, 259–270.
- Johnson, P., 1994. Historical Assessment of Elwha River Fisheries. Draft Report to the U.S. National Park Service, Olympic National Park, WA, p. 355.
- Jones, J.I., Murphy, J.F., Collins, A.L., Sear, D.A., Naden, P.S., Armitage, P.D., 2012. The impact of fine sediment on macro-invertebrates. *River Res. Appl.* 28, 1055–1071.
- Juracek, K.E., Fitzpatrick, F.A., 2009. Geomorphic applications of stream-gage information. *River Res. Appl.* 25, 329–347. <http://dx.doi.org/10.1002/rra.1163>.
- Kaller, M.D., Hartman, K.J., 2004. Evidence of threshold level of fine sediment accumulation for altering benthic macroinvertebrate communities. *Hydrobiologia* 518, 95–104.
- Karssenberg, D., Bridge, J.S., 2008. A three-dimensional numerical model of sediment transport, erosion and deposition within a network of channel belts, floodplain and hill slope: extrinsic and intrinsic controls on floodplain dynamics and alluvial architecture. *Sedimentology* 55, 1717–1745.
- Kibler, K.M., Tullus, D.D., 2013. Cumulative biophysical impact of small and large hydro-power development in Nu River, China. *Water Resour. Res.* 49, 3104–3118.
- Kloehn, K.K., Beechie, T.J., Morley, S.A., Coe, H.J., Duda, J.J., 2008. Influence of dams on river-floodplain dynamics in the Elwha River, Washington. *Northwest Sci.* 82 (Special Issue), 224–235.
- Knighton, A.D., 1989. River adjustment to changes in sediment load: the effects of tin mining on the Ringarooma River, Tasmania, 1875–1984. *Earth Surf. Process. Landf.* 14, 333–359.
- Knighton, A.D., Nanson, G.C., 1993. Anastomosis and the continuum of channel pattern. *Earth Surf. Process. Landf.* 18, 613–625.
- Kocovsky, P.M., Ross, R.M., Dropkin, D.S., 2009. Prioritizing removal of dams for passage of diadromous fishes on a major river system. *River Res. Appl.* 25, 107–117.
- Kondolf, G.M., Wolman, M.G., 1993. The sizes of salmonid spawning gravels. *Water Resour. Res.* 29, 2275–2285.

- Kondolf, G.M., Piegay, H., Landon, N., 2002. Channel response to increased and decreased bedload supply from land use change: contrasts between two catchments. *Geomorphology* 45, 35–51.
- Kondolf, G.M., Rubin, Z.K., Minear, J.T., 2014. Dams on the Mekong: cumulative sediment starvation. *Water Resour. Res.* 50. <http://dx.doi.org/10.1002/2013WR014651>.
- Konrad, C.P., 2009. Simulating the recovery of suspended sediment transport and riverbed stability in response to dam removal on the Elwha River, Washington. *Ecol. Eng.* 35, 1104–1115.
- Lane, S.N., Westaway, R.M., Hicks, D.M., 2003. Estimation of erosion and deposition volumes in a large, gravel-bed, braided river using synoptic remote sensing. *Earth Surf. Process. Landf.* 28, 249–271.
- Latterell, J.J., Bechtold, J.S., O'Keefe, T.C., Van Pelt, R., 2006. Dynamic patch mosaics and channel movement in an unconfined river valley of the Olympic Mountains. *Freshw. Biol.* 51, 523–544.
- Lauer, J.W., Parker, G., Dietrich, W.E., 2008. Response of the Strickland and Fly River confluence to postglacial sea level rise. *J. Geophys. Res.* 113 (F01S06). <http://dx.doi.org/10.1029/2006JF000626>.
- Leopold, L.B., Maddock, T.J., 1953. The hydraulic geometry of stream channels and some physiographic implications. *U. S. Geol. Surv. Prof. Pap.* 252, 57.
- Ligon, F.K., Dietrich, W.E., Trush, W.J., 1995. Downstream ecological effects of dams. *Bioscience* 45, 183–192.
- Lisle, T.E., 1989. Sediment transport and resulting deposition in spawning gravels, north coastal California. *Water Resour. Res.* 25, 1303–1319.
- Lisle, T.E., 2008. The evolution of sediment waves influenced by varying transport capacity in heterogeneous rivers. In: Habersack, H., Piegay, H., Rinaldi, M. (Eds.), *Gravel Bed Rivers VI: From Process Understanding to River Restoration*. Elsevier, Amsterdam, pp. 443–472. [http://dx.doi.org/10.1016/S0928-2025\(07\)11136-6](http://dx.doi.org/10.1016/S0928-2025(07)11136-6).
- Lisle, T.E., Pizzuto, J.E., Ikeda, H., Iseya, F., Kodama, Y., 1997. Evolution of a sediment wave in an experimental channel. *Water Resour. Res.* 33, 1971–1981. <http://dx.doi.org/10.1029/97WR01180>.
- Lisle, T.E., Cui, Y., Parker, G., Pizzuto, J.E., Dodd, A.M., 2001. The dominance of dispersion in the evolution of bed material waves in gravel-bed rivers. *Earth Surf. Process. Landf.* 26, 1409–1420. <http://dx.doi.org/10.1002/esp.300>.
- Lyons, J.K., Beschta, R.L., 1983. Land use, floods, and channel changes—Upper Middle Fork Willamette River, Oregon (1936–1980). *Water Resour. Res.* 19, 463–471.
- Madej, M.A., Ozaki, V., 1996. Channel response to sediment wave propagation and movement, Redwood Creek, California, USA. *Earth Surf. Process. Landf.* 21, 911–927.
- Madej, M.A., Sutherland, D.G., Lisle, T.E., Prior, B., 2009. Channel responses to varying sediment input: a flume experiment modeled after Redwood Creek, California. *Geomorphology* 103, 507–519.
- Magilligan, F.J., Nislow, K.H., 2005. Changes in hydrologic regime by dams. *Geomorphology* 71, 61–78.
- Magirl, C.S., Curran, C.A., Sheibley, R.W., Warrick, J.A., Czuba, J.A., Czuba, C.R., Gendaszek, A.S., Shafroth, P.B., Duda, J.J., Foreman, J.R., 2011. Baseline hydrologic studies in the lower Elwha River prior to dam removal. In: Duda, J.J., Warrick, J.A., Magirl, C.S. (Eds.), *Coastal Habitats of the Elwha River, Washington—Biological and Physical Patterns and Processes Prior to Dam Removal*. U.S. Geol. Surv. Sci. Investig. Rep. 2011-5120, 75–110.
- Magirl, C.S., Hilldale, R.C., Curran, C.A., Duda, J.J., Straub, T.D., Domanski, M., Foreman, J.R., 2014. Large-scale dam removal on the Elwha River, Washington, USA: Fluvial sediment load. *Geomorphology* (in this volume).
- Major, J.J., O'Connor, J.E., Podolak, C.J., Keith, M.K., Grant, G.E., Spicer, K.R., Pittman, S., Bragg, H.M., Wallick, J.R., Tanner, D.Q., Rhode, A., Wilcock, P.R., 2012. Geomorphic response of the Sandy River, Oregon, to removal of Marmot Dam. *U. S. Geol. Surv. Prof. Pap.* 1792 (64 pp.).
- McHenry, M.L., Pess, G.R., 2008. An overview of monitoring options for assessing the response of salmonids and their aquatic ecosystems in the Elwha River following dam removal. *Northwest Sci.* 82 (Special Issue), 29–47.
- McHenry, M., Pess, G., Abbe, T., Coe, H., Goldsmith, J., Liermann, M., McCoy, R., Morley, S., Peters, R., 2007. The physical and biological effects of engineered logjams (ELJs) in the Elwha River, Washington. Report to Salmon Recovery Funding Board and Interagency Committee for Outdoor Recreation, Port Angeles, WA, p. 82.
- Merritt, D.M., Cooper, D.J., 2000. Riparian vegetation and channel change in response to river regulation: a comparative study of regulated and unregulated streams in the Green River Basin, USA. *Regul. Rivers Res. Manag.* 16, 543–564.
- Meyer, D.F., Martinson, H.A., 1989. Rates and processes of channel development and recovery following the 1980 eruption of Mount St. Helens, Washington. *Hydrolog. Sci. J.* 34, 115–127.
- Milan, D.J., Heritage, G.L., Large, A.R., Fuller, I.C., 2011. Filtering spatial error from DEMs: implications for morphological change estimation. *Geomorphology* 125, 160–171.
- Miller, D.J., Benda, L.E., 2000. Effects of punctuated sediment supply on valley-floor landforms and sediment transport. *Geol. Soc. Am. Bull.* 112, 1814–1824.
- Minshall, G.W., Royer, T.V., Robinson, C.T., 2001. Response of the Cache Creek macroinvertebrates during the first 10 years following disturbance by the 1988 Yellowstone wildfires. *Can. J. Fish. Aquat. Sci.* 58, 1077–1088.
- Mohrig, D.M., Heller, P.L., Paola, C., Lyons, W.J., 2000. Interpreting avulsion processes from ancient alluvial sequences: Guadalupe-Matarranya system (northern Spain) and Wasatch Formation (western Colorado). *Geol. Soc. Am. Bull.* 112, 1787–1803.
- Montgomery, D.R., Panfil, M.S., Hayes, S.K., 1999. Channel-bed mobility response to extreme sediment loading at Mount Pinatubo. *Geology* 27, 271–274.
- Morley, S.A., Duda, J.J., Coe, H.J., Kloehn, K.K., McHenry, M.L., 2008. Benthic invertebrates and periphyton in the Elwha River basin: current conditions and predicted response to dam removal. *Northwest Sci.* 82 (Special Issue), 179–196.
- Mossop, Bradford, 2006. Using thalweg profiling to assess and monitor juvenile salmon (*Oncorhynchus* spp.) habitat in small streams. *Can. J. Fish. Aquat. Sci.* 63, 1515–1525.
- Mueller, E.R., Pitlick, J., 2013. Sediment supply and channel morphology in mountain river systems: 1. Relative importance of lithology, topography, and climate. *J. Geophys. Res. Earth Surf.* 118, 2325–2342.
- Naiman, R.J., Bechtold, J.S., Beechie, T.J., Latterell, J.J., Van Pelt, R., 2010. A process-based view of floodplain forest patterns in coastal river valleys of the Pacific Northwest. *Ecosystems* 13, 1–13.
- Nanson, G.C., Croke, J.C., 1992. A genetic classification of floodplains. *Geomorphology* 4, 459–486.
- Nicholas, A.P., Ashworth, P.J., Kirkby, M.J., Macklin, M.G., Murray, T., 1995. Sediment slugs: large-scale fluctuations in fluvial sediment transport rates and storage volumes. *Prog. Phys. Geogr.* 19 (4), 500–519.
- O'Connor, J.E., Jones, M.A., Haluska, T.L., 2003. Flood plain and channel dynamics of the Quinalt and Queets Rivers, Washington, USA. *Geomorphology* 51, 31–59.
- Pearson, A.J., Snyder, N.P., Collins, M., 2011. Rates and processes of channel response to dam removal with a sand-filled impoundment. *Water Resour. Res.* 47, W08504. <http://dx.doi.org/10.1029/2010WR009733>.
- Pess, G.R., McHenry, M.L., Beechie, T.J., Davies, J., 2008. Biological impacts of the Elwha River dams and potential salmonid responses to dam removal. *Northwest Sci.* 82 (Special Issue), 72–90.
- Pierson, T.C., Major, J.J., 2014. Hydrogeomorphic effects of explosive volcanic eruptions on drainage basins. *Ann. Rev. Earth Planet. Sci.* 42, 469–507.
- Pierson, T.C., Pringle, P.T., Cameron, K.A., 2011. Magnitude and timing of downstream channel aggradation and degradation in response to a dome-building eruption at Mount Hood, Oregon. *Geol. Soc. Am. Bull.* 123, 3–20. <http://dx.doi.org/10.1130/B30127.1>.
- Pitlick, J., 1993. Response and recovery of a subalpine stream following a catastrophic flood. *Geol. Soc. Am. Bull.* 105 (5), 657–670. [http://dx.doi.org/10.1130/0016-7606\(\(1993\)105:0657:raoas>2.3.co;2\)](http://dx.doi.org/10.1130/0016-7606((1993)105:0657:raoas>2.3.co;2).
- Pizzuto, J.E., 2002. Effects of dam removal on river form and process. *Bioscience* 52, 683–691.
- Podolak, C.J.P., Wilcock, P.R., 2013. Experimental study of the response of a gravel streambed to increased sediment supply. *Earth Surf. Process. Landf.* 38, 1748–1764.
- Poff, N.L., Hart, D.D., 2002. How dams vary and why it matters for the emerging science of dam removal. *Bioscience* 52, 659–668.
- Pohl, M., 2004. Channel bed mobility downstream from the Elwha dams, Washington. *Prof. Geogr.* 56 (3), 422–431.
- Polenz, M., Wegmann, K.W., Schasse, H.W., 2004. Geologic map of the Elwha and Angeles Point 7.5-minute quadrangles, Clallam County, Washington. Open-File Report 2004-14, scale 1:24,000, Washington Division of Geology and Earth Resources, Olympia, WA.
- Pryor, B.S., Lisle, T.E., Montoya, D.S., Hilton, S., 2011. Transport and storage of bed material in a gravel-bed channel during episodes of aggradation and degradation: a field and flume study. *Earth Surf. Process. Landf.* 36, 2028–2041.
- Randle, T.J., Young, C.A., Melena, J.T., Ouellette, E.M., 1996. Sediment analysis and modeling of the river erosion alternative. U.S. Bureau of Reclamation, Pacific Northwest Region, Elwha Technical Series PN-95-9, p. 138.
- Randle, T.J., Bountry, J.A., Ritchie, A., Wille, K., 2014. Large-scale dam removal on the Elwha River, Washington, USA: erosion of reservoir sediment. *Geomorphology* (in this volume).
- Rantz, S.E., 1982. Measurement and computation of streamflow—volume 2, computation of discharge. U.S. Geol. Surv. Water Supply Pap. 2175, 376.
- Renwick, W.H., Smith, S.V., Bartley, J.D., Buddeimer, R.W., 2005. The role of impoundments in the sediment budget of the conterminous United States. *Geomorphology* 71, 99–111.
- Riebe, C.S., Sklar, L.S., Overstreet, B.T., Wooster, J.K., 2014. Optimal reproduction in salmon spawning substrates linked to grain size and fish length. *Water Resour. Res.* 50, 898–918. <http://dx.doi.org/10.1002/2013WR014231>.
- Rubin, D.M., 2004. A simple autocorrelation algorithm for determining grain size from digital images of sediment. *J. Sediment. Res.* 74, 160–165.
- Sawaske, S.R., Freyberg, D.L., 2012. A comparison of past small dam removals in highly sediment-impacted systems in the U.S. *Geomorphology* 151–152, 50–58.
- Schmidt, J.C., Graf, J.B., 1990. Aggradation and degradation of alluvial sand deposits, 1965 to 1986, Colorado River, Grand Canyon National Park, Arizona. *U. S. Geol. Surv. Prof. Pap.* 1493, 74.
- Schmidt, J.C., Wilcock, P.R., 2008. Metrics for assessing the downstream effects of dams. *Water Resour. Res.* 44, W04404. <http://dx.doi.org/10.1029/2006WR005092>.
- Schumm, S.A., 1985. Patterns of alluvial rivers. *Ann. Rev. Earth Planet. Sci.* 13, 5–27.
- Service, R.F., 2011. Will busting dams boost salmon? *Science* 334, 888–892.
- Shafroth, P.B., Stromberg, J.C., Patten, D.T., 2002a. Riparian vegetation response to altered disturbance and stress regimes. *Ecol. Appl.* 12, 107–123.
- Shafroth, P.B., Friedman, J.M., Auble, G.T., Scott, M.L., Braatne, J.H., 2002b. Potential responses of riparian vegetation to dam removal. *Bioscience* 52, 703–712.
- Simon, A., 1999. Channel and drainage-basin response of the Toutle River system in the aftermath of the 1980 eruption of Mount St. Helens, Washington. *U.S. Geological Survey Open-file Report 96-633*, p. 130.
- Simons, R.K., Simons, D.B., 1991. Sediment problems associated with dam removal—Muskegon River, Michigan. In: Shane, R.M. (Ed.), *Hydraulic Engineering. Proceedings of the National Conference on Hydraulic Engineering*. American Society of Civil Engineers, New York, pp. 680–685.
- Sinha, R., 2009. The great avulsion of Kosi on 18 August 2008. *Curr. Sci.* 97, 429–433.
- Sklar, L.S., Fadde, J., Venditti, J.G., Nelson, P., Wydżga, M.A., Cui, Y., Dietrich, W.E., 2009. Translation and dispersion of sediment pulses in flume experiments simulating gravel augmentation below dams. *Water Resour. Res.* 45, W08439. <http://dx.doi.org/10.1029/2008WR007346>.
- Slingerland, R., Smith, N.D., 1998. Necessary conditions for a meandering-river avulsion. *Geology* 26, 435–438.

- Slingerland, R., Smith, N.D., 2003. River avulsions and their deposits. *Annu. Rev. Earth Planet. Sci.* 32, 257–285.
- Smelser, M.G., Schmidt, J.C., 1998. An assessment methodology for determining historical changes in mountain streams. General Technical Report RMRS-GTR-6. U.S. Department of Agriculture—U.S. Forest Service Rocky Mountain Research Station, Fort Collins, Colorado, p. 29.
- Smith, N.D., Smith, D.G., 1984. William River: an outstanding example of channel widening and braiding caused by bed-load addition. *Geology* 12, 78–82.
- Snavely, S.N., Seitz, S.M., Szeliski, R., 2008. Modeling the world from Internet photo collections. *Int. J. Comput. Vis.* 80, 189–210.
- Stanley, E.H., Luebke, M.A., Doyle, M.W., Marshall, D.W., 2002. Short-term changes in channel form and macroinvertebrate communities following low-head dam removal. *J. N. Am. Benthol. Soc.* 21, 172–187.
- Sutherland, D.G., Ball, M.H., Hilton, S.J., Lisle, T.E., 2002. Evolution of a landslide-induced sediment wave in the Navarro River, California. *Geol. Soc. Am. Bull.* 114 (8), 1036–1048.
- Svitiksi, J.P.M., Vörösmarty, C.J., Kettner, A.J., Green, P., 2005. Impact of humans on the flux of terrestrial sediment to the global coastal ocean. *Science* 308, 376–380.
- Tabor, R.W., Cady, W.M., 1978. Geologic map of the Olympic Peninsula, Washington. U.S. Geological Survey Miscellaneous Investigations Series Map I-944, 2 sheets, scale 1: 125,000, Reston, VA.
- Tal, M., Paola, C., 2010. Effects of vegetation on channel morphodynamics: results and insights from laboratory experiments. *Earth Surf. Process. Landf.* 35, 1014–1028.
- Taylor, J.R., 1997. An Introduction to Error Analysis. University Science Books, Sausalito, California, p. 327.
- Thompson, J.R., Hart, D.D., Charles, D.F., Nightengale, T.L., Winter, D.M., 2005. Effects of removal of a small dam on downstream macroinvertebrate and algal assemblages in a Pennsylvania stream. *J. N. Am. Benthol. Soc.* 24, 192–207.
- Tullos, D., Wang, H.-W., 2014. Morphological responses and sediment processes following a typhoon-induced dam failure, Dahan River, Taiwan. *Earth Surf. Process. Landf.* 39, 245–258.
- Tullos, D.D., Cox, M.M., Walter, C., Kibler, K.M., 2010. Processing of sediment pulses following the removal of three small, gravel-filled barriers. American Geophysical Union, Fall Meeting 2010, Abstract H34B-01, San Francisco, CA.
- U.S. Department of Interior, 1996a. Removal of Elwha and Glines Canyon Dams. U.S. Bureau of Reclamation, Elwha Technical Series PN-95-7, p. 86.
- U.S. Department of Interior, 1996b. Environmental Impact Statement (EIS-2): Implementation EIS. Elwha River Ecosystem Restoration Implementation Final Environmental Impact Statement. National Park Service, U.S. Fish and Wildlife Service, U.S. Bureau of Reclamation, U.S. Bureau of Indian Affairs, U.S. Army Corps of Engineers, and Lower Elwha Klallam Tribe, (<http://federalregister.gov/a/04-25356>).
- Vinson, M.R., 2001. Long-term dynamics of an invertebrate assemblage downstream from a large dam. *Ecol. Appl.* 11, 711–730.
- Wang, Y., Straub, K.M., Hajek, E.A., 2011. Scale dependent compositional stacking: an estimate of autogenic timescales in sedimentary deposits. *Geology* 39, 811–814.
- Warrick, J.A., Rubin, D.M., Ruggiero, P., Harney, J.N., Draut, A.E., Buscombe, D., 2009. Cobble Cam: grain-size measurements of sand to boulder from digital photographs and autocorrelation analyses. *Earth Surf. Process. Landf.* 34, 1811–1821.
- Warrick, J.A., Draut, A.E., McHenry, M.L., Miller, I.M., Magirl, C.S., Beirne, M.M., Stevens, A. W., Logan, J.B., 2011. Geomorphology of the Elwha River and its delta. In: Duda, J.J., Warrick, J.A., Magirl, C.S. (Eds.), US Geol. Surv. Sci. Investig. Rep. 2011-5120-3, 47–74.
- Warrick, J.A., Duda, J.J., Magirl, C.S., Curran, C.A., 2012. River turbidity and sediment loads during dam removal. *Eos* 93, 425–426.
- Warrick, J.A., Bountry, J.A., East, A.E., Magirl, C.S., Randle, T.J., Gelfenbaum, G.R., Ritchie, A.C., Pess, G.R., Leung, V., Duda, J.J., 2014. Large-scale dam removal on the Elwha River, Washington, USA: source-to-sink sediment budget and synthesis. *Geomorphology* (in this volume).
- Westoby, M.J., Brasington, J., Glasser, N.F., Hambrey, M.J., Reynolds, J.M., 2012. Structure-from-Motion photogrammetry: a low-cost, effective tool for geoscience applications. *Geomorphology* 179, 300–314.
- Wheaton, J.M., Brasington, J., Darby, S.E., Sear, D.A., 2010. Accounting for uncertainty in DEMs from repeat topographic surveys: improved sediment budgets. *Earth Surf. Process. Landf.* 35, 136–156.
- Wilcox, A.C., O'Connor, J.E., Major, J.J., 2014. Rapid reservoir erosion, hyperconcentrated flow, and downstream deposition triggered by breaching of 38-m-tall Condit Dam, White Salmon River, Washington. *J. Geophys. Res. Earth Surf.* <http://dx.doi.org/10.1002/2013JF003073>.
- Williams, G.P., Wolman, M.G., 1984. Effects of dams and reservoirs on surface-water hydrology: changes in rivers downstream from dams. U. S. Geol. Surv. Prof. Pap. 1286 (83 pp.).
- Wing, S., 2014. Reservoir sediment carbon along the Elwha River after dam removal (M.S. thesis) School of Environmental and Forest Sciences. University of Washington, Seattle, p. 68.
- Woelfle-Erskine, C., Wilcox, A.C., Moore, J.N., 2012. Combining historic and process perspectives to infer ranges of geomorphic variability and inform river restoration in a wandering gravel-bed river. *Earth Surf. Process. Landf.* 37, 1302–1312.
- Wohl, E., 2013. Floodplains and wood. *Earth Sci. Rev.* 123, 194–212.
- Wohl, E.E., Cenderelli, D.A., 2000. Sediment deposition and transport patterns following a reservoir sediment release. *Water Resour. Res.* 36, 319–333.
- Wolman, M.G., 1954. A method of sampling coarse river-bed material. *Trans. Am. Geophys. Union* 35, 951–956.
- Wood, P.J., Armitage, P.D., 1997. Biological effects of fine sediment in the lotic environment. *Environ. Manag.* 21, 203–217.
- Wunderlich, R.C., Winter, B.D., Meyer, J.H., 1994. Restoration of the Elwha River ecosystem. *Fisheries* 19 (8), 11–19.
- Xu, X., Tan, Y., Yang, G., 2013. Environmental impact assessments of the Three Gorges Project in China: issues and interventions. *Earth Sci. Rev.* 124, 115–125.
- Zhou, J., Zhang, M., Lu, P., 2013. The effects of dams on phosphorous in the middle and lower Yangtze river. *Water Resour. Res.* 49, 3659–3669.